Manuscript type: Research article

Assessing Landslide Damming susceptibility in Central Asia

Carlo Tacconi Stefanelli[a,b,*], William Frodella[a,b], Francesco Caleca[a,b], Zhanar Raimbekova[c,d], Ruslan Umuraliev[e], Veronica Tofani[a,b]

[a] University of Florence, Department of Earth Sciences, via G. la Pira 4, 50121 Florence, Italy

[b] UNESCO Chair on the Prevention and Sustainable Management of Geo-Hydrological Hazards, University of Florence, Largo Fermi 2, 50125 Florence, Italy

[c] Institute of Seismology of Republic of Kazakhstan (IS), Almaty, Kazakhstan

[d] Al-Farabi Kazakh National University, Department of Geography and Environmental Sciences, Al-Farabi ave. 71, A15E3C7 Almaty, Kazakhstan

[e] Institute of Seismology of the National Academy of Sciences of Kyrgyz Republic (ISNASKR), Bishkek, Kyrgyz Republic

* *Correspondence to*: carlo.tacconistefanelli@unifi.it

Abstract

Central Asia regions are characterized by active tectonics, high mountain chains with extreme topography with glaciers and strong seasonal rainfall events. These key predisposing factors make large landslides a serious natural threat in the area, causing several casualties every year. The mountain crests are divided by wide lenticular or narrow, linear intermountain tectonic depressions, which are incised by many of the most important Central Asia rivers and are also subject to major seasonal river flood hazard. This multi-hazard combination is a source of potential damming scenarios which can bring cascading effects with devastating consequences for the surrounding settlements and population. Different hazards can only be managed with a multi-hazard approach coherent within the different countries, as suggested by the requirements of the Sendai Framework for Disaster Risk Reduction.

This work was carried out within the framework of the SFRARR Project ("*Strengthening Financial Resilience and Accelerating Risk Reduction in Central Asia*") as a part of a multi-hazard approach with the aim of providing a damming susceptibility analysis at a regional scale for Central Asia. To achieve this, a semi-automated GIS-based mapping method, centred on a bivariate correlation of morphometric parameters defined by a morphological index, originally designed to assess the damming susceptibility at basin/regional scale, was modified to be adopted nationwide and applied to spatially assess the obstruction of the river network in Central Asia for mapped and newly formed landslides. The proposed methodology represents an improvement of the previously designed, requiring a smaller amount of data, bringing new preliminary information on the damming hazard management and risk reduction identifying the most critical area within the Central Asia regions.

1 Introduction

The mountainous areas of the Djungaria, Tien Shan, Pamir and Kopetdag in Central Asia territories are characterized by complex and active tectonic and are the sources of most of Central Asia rivers. A rugged topography along with complex geological structure and high seismicity are ideal setting for large slope failures. In general, when landslides completely obstruct a river channel, they generate a landslide dam whose consequences can be a serious hazard forming upstream backwater and causing catastrophic downstream flooding, changes in the riverbed, embankments instability triggering other landslides with a cascading effect (Swanson et al., 1986; Costa and Schuster, 1988; Casagli and Ermini,1999). The effects of impounded water and anomalous flood waves, resulting from a dam breach, have significant economic and social impacts in upstream and downstream areas with economic and human losses (King et al., 1989; Dai et al., 2005; Chen and Chang, 2016). Rebuilding costs can be extensive, as they are direct (e.g., infrastructure and buildings reconstruction, safety measures) and indirect (e.g., loss in real estate value and damage caused to industrial and agricultural production), harder to estimate.

Most of landslide dams have a short life as about 40% of them collapse within 24 hours after formation and about 80% within one year (Costa and Schuster, 1988; Tacconi Stefanelli et al., 2015; Fan et al., 2020). Given the limited available time, a complete and reliable analysis of the risks, requiring in-depth study of the phenomenon, is not achievable during the event and only rapid assessments for the dam stability are suitable. When the people to evacuate are too many or the related risk is too high, engineering measures for the hazard reduction are attempted: among these are for example modification of slope geometry, drainage, retaining structures and internal slope reinforcement (Popescu and Sasahara, 2009; Schuster and Evans, 2011). Therefore, part of the effects from landslide damming can be avoided or at least reduced thanks to mitigation and prevention measures (e.g., slopes stabilization or re-profiling) if the most critical areas with the highest damming probability are known. Consequently, planning and prevention tools, such as risk and susceptibility mapping, are essential to reduce the costs of natural hazard and improve the efficiency of environmental management.

Reactivation of ancient landslides triggered during different climatic and environmental conditions may often generate new mass movements (Casagli and Ermini, 1999; Canuti et al., 2004; Dikau and Schrott, 1999; Borgatti and Soldati, 2010; Crozier, 2010). Landslides generated in the past are often dormant, with strength parameters of the sliding surface close to the residual ones, and difficult to recognize because vegetation, erosion and superficial alteration hide their morphology. Natural causes, such as earthquakes, river undercutting, rainfall, and snowmelt, or even anthropic activity can reactivate these ancient phenomena. Therefore, all dormant landslides capable to reach a river along their pathway can potentially dam it and should be investigated. New landslides, instead, may develop wherever are present suitable conditions along the slopes. The spatial occurrence probability is commonly assessed by landslide susceptibility analysis, highly dependent on landslide volume (Catani et al., 2016), which is difficult to accurately predict.

Landslides in Central Asia are quite common and a considerable number of them have huge dimension, often induced by strong earthquakes but also by floods, heavy rainfall and snowmelt (Behling et al., 2014; Golovko et al., 2015; Havenith et al., 2015a; 2015b; 2006b; Kalmetieva et al., 2009; Rosi et al., 2023; Saponaro et al., 2014; Strom and Abdrakhmatov, 2017; 2018). Concerning landslide dam events, in Central Asia regions several mass movements of considerable size produced the obstruction of a river section, of which more than 100 still are existing with a lake (Strom, 2010). Although many of these could be considered stable (Strom, 2010), the occurrence of devastating outburst floods in the last century show that their potential hazard should never be overlooked also considering the seismicity of the region. In the Rushan and Murgab districts of Gorno-Badakhshan Autonomous Oblast (Pamirs, Tajikistan) along the Murghab river, the Usoi landslide dam is one of the most famous of the many cases in the regions. Its impounded lake, called Lake Sarez, is 60 km long with 500 m of depth and has a stored volume of about 17 km^3, representing the world deepest landslide-dammed lake (Costa and Schuster, 1991; Fan et al., 2020). It was originated on February 18th, 1911, when a MW 7.2 earthquake triggered a giant wedge-failure of about 2.2 km^3 of rock (mainly quartzite, schist, shale and dolomite) and debris that blocked the Murgab River and a tributary valley, forming the 560 m high, 5 km long and 4 km wide Usoi dam, impounding Lake Sarez, also creating the smaller Lake Shadau (Strom, 2010).

Landslide dam evolution, according to some studies (Swanson et al., 1986; Ermini and Casagli, 2003; Dal Sasso et al., 2014; Tacconi Stefanelli et al., 2016), can be estimated through geomorphological indexes which require parameters characterizing the landslide (or the dam) and the river (or the lake). Geomorphological indexes are a powerful classification tool, but their prediction power depend mainly on long studies, a large amount of data and measurement efforts given their empirical nature. Many of these indexes need parameters not always available and easy to acquire, such as grain size distribution (Liao et al., 2022) or landslide velocity (Swanson et al., 1986).

In this work, we propose a simple semi-automatic GIS-based mapping methodology to verify the damming susceptibility of river networks at national scale from existing and neo-formed landslides trough a geomorphological index. This activity research was carried out in the framework of the SFRARR Project ("*Strengthening Financial Resilience and Accelerating Risk Reduction in Central Asia*") as a part of a multi-hazard approach (Peresan et al., 2023).

The proposed mapping methodology represents an innovation in terms of application simplicity, availability of data and of extension of the analysed area, bringing new information on the damming hazard in the Central Asia regions where the landslide susceptibility is quite high (Rosi et al., 2023) and a set of input data required for the methodology application were available.

2 Study area

Central Asia is a region of vast diversity encompassing high mountain chains, deserts, and steppes (Figure 1). The southern and eastern parts of the region are predominantly occupied by the mountainous areas of Djungaria, Tien Shan, Pamir, Kopetdag, and a small part of Western Altaj, with peaks exceeding 7,000 m above sea level (a.s.l) (Strom, 2010). These intraplate mountain systems, developed in the Cenozoic as a result of the India-Asian collision, is located between the Tarim Basin and the Kazakh Shield (Molnar and Tapponier 1975, Abdrakhmatov et al., 1996; 2003; Zubovich et al., 2010; Ullah et al., 2015). This study focusses the attention on the territories of Central Asia that includes Turkmenistan, Kazakhstan, Kyrgyz Republic, Uzbekistan, and Tajikistan, covering a surface of more than $4 \cdot 10^6$ km^2. Mountain building began in the Oligocene (Chedia, 1980) or later (Abdrakhmatov et al., 1996), resulting in a complex system of basement folds interrupted by several thrusts and reverse faults with lateral offset of important amounts (Delvaux et al., 2001).

Figure 1. Geographical framework of the study area. Lake's polygons from Esri, Garmin International, Inc.; topographic base from NASA's SRTM project (Farr and Kobrick, 2000).

The mountain belts contain several regional fault zones (Figure 2), and others cross the mountain systems with a NW-SE axis (Trifonov et al., 1992). Paleozoic crystalline rocks form, for the most part, the mountain ridges which correspond to a neotectonic anticline and are separated by tectonic depressions, with lenticular or linear shapes. These intermountain depressions host the primary river valleys and are filled by Neogene and Quaternary deposits, principally sandstones, siltstones interbedded by gypsum, and conglomerates (Strom and Abdrakhmatov, 2017). Lithologies from Mesozoic and Paleogene are characteristic of the areas at the foot of mountain ranges (Figure 2). This main deeply incised river network, fed by glaciers, snowmelt water and rain, is linked by narrow deep gorges up to 1-2 km deep (Strom and Abdrakhmatov, 2018) and is the origin of most of the rivers in Central Asia.

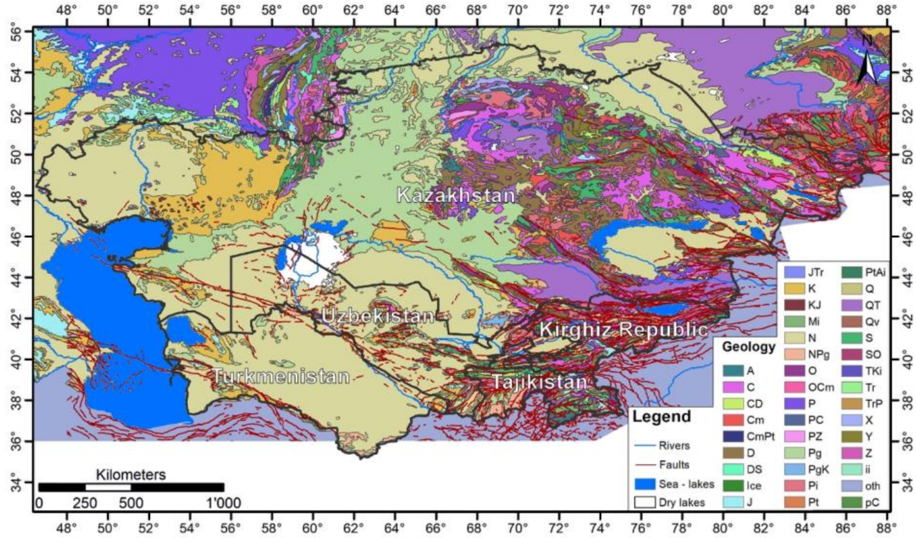

Figure 2. Geological map of the area. Geological formation data are from the United States Geological Survey (USGS) (Persits et al., 1997, https://doi.org/10.3133/ofr97470E, for the legend), faults are from the Active Faults of Eurasia Database (AFEAD) (Styron and Pagani, 2020, https://doi.org/10.1177/8755293020944182).

The retreat and shrinkage of glaciers in Central Asia regions induced by the global warming produce a seasonal variation in river discharge and consequently an increase of its induced hazards such as Glacial Lake Outburst Floods (GLOFs) (Falátková, 2016), resulting in countless losses of human life and destroyed infrastructure (Kropáček et al., 2021; Petrov et al., 2017; Wang et al., 2013). The high seismicity, frequent floods and a complex geological and topographical structure (such as lithological predisposition, faulting zones, steep slopes) contribute to predispose the region to frequent landslides which can potentially obstruct the narrow valleys of the mountain ranges and in turn be the cause of chain risks (CAC DRMI, 2009; Havenit et al., 2017).

3 Materials and Methods

The Morphological Obstruction Index (MOI) (Tacconi Stefanelli et al., 2016) is a bivariate index able to evaluate the potential hazard posed by landslide dams that requires only simple morphometrical parameters which are easily extracted from common Digital Elevation Models. The MOI is based on the interpolation of 351 documented cases and has been used in several studies, such as in Italy and Peru (Tacconi Stefanelli et al., 2016; 2018), to assess landslide damming susceptibility showing better results than others popular indexes (Swanson et al., 1986). This empirical index is a useful tool for identifying high-risk areas and for prioritizing mitigation efforts in landslide-prone regions.

The MOI is calculated by dividing the volume of the landslide, V_l (m^3), by the width of the river valley, W_v (m), at the dam location.

$$MOI = log\left({}^{V_l}/_{W_v}\right) \tag{1}$$

The MOI is based on the principle that the higher the ratio of the landslide volume to the river width, the greater the potential for dam formation. It is important to point out that river width, W_v, shall be defined as the width of the river valley which can potentially be obstructed creating a dammed lake and not of just the channel where the river flows, as is often misinterpreted, although in narrow mountain valleys these often coincide.

Landslide dams analyzed by the index can be grouped within three evolutionary classes: formed (the red area, where the plotted landslides have completely blocked their river), not formed (the blue area, where only cases of unobstructed rivers are found) and of uncertain evolution (the purple area, in which both cases of formed and unformed dam can be found). The limits of these domains are depicted by two lines, the lower red “Non-formation line” and the upper blue “Formation line” (Figure 3) obtained by the interpolation of the cases analyzed by Tacconi Stefanelli et al. (2018).

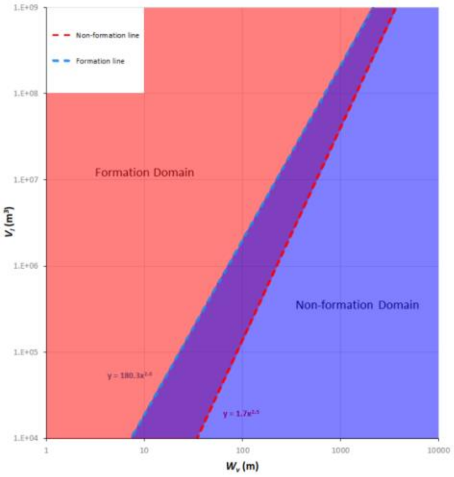

Figure 3. Schematic plot of the non-Formation line and Formation line.

The equation of the former is expressed as follows:

$$V_l' = 1.7 \cdot W_v^{2.5} \tag{2}$$

Where V_l’ is the “Non-formation volume” and is the minimum landslide volume able to potentially block a river with a given width W_v. Smaller volumes cannot completely dam the river. The latter expression draws the upper limit for not formed dams and is expressed as follows:

$$V_l'' = 180.3 \cdot W_v^2 \tag{3}$$

Where V_l’’ is the “Formation volume”, is the minimum landslide volume able to dam the river valley, with a confidence of 99%, and the inferior boundary of the Formation domain (which includes only formed dams).

Intermediate cases that fall between the two lines cannot be confidently identified as formed or unformed and are therefore classified as having uncertain evolution.

As originally proposed by Tacconi Stefanelli et al. (2020), these two equations, Eq.(2) and (3), can be used to apply a simple semi-automatic methodology in order to verify at basin scale the damming susceptibility from existing and neo-formed landslides. The following semi-automated procedure, inspired by the one of Tacconi Stefanelli et al. (2020) of which this represents an improvement, is applied on a national scale and can be reproduced entirely in a GIS (Geographic Information System) environment. However, the method, being initially designed for analysis at basin/region scale, applied to such a small scale (national) will not be able to provide detailed information. For this reason, this study represents a preliminary phase of investigation which will allow to concentrate further detailed analysis on the areas identified as more critical.

Within an even medium-long time interval the valley width in each river stretch does not change significantly and can be considered an immutable factor in the MOI equation (Eq.(1)). Starting from this assumption, along with Eq. (2) and Eq. (3), if the average river width W_v of each river stretch can be assessed, the two threshold landslide volumes V_l’ (Non-formation volume) and V_l’’ (Formation volume) can be estimated for each river stretch.

Landslides that cause river obstruction are in many cases reactivations of ancient movements that are still in a condition of partial instability and that have not reached a potential equilibrium reaching the valley floor. Therefore, with a landslide inventory it is possible to assess, with some assumptions and simplifications, which among the mapped landslides are able to dam the river section. Each landslide that is not already laying in the valley floor with a volume bigger than V' and V" are identified as potentially prone to block the river in the future in that point. Then, a "Map of Damming Susceptibility" for reactivation of existing landslides can be generated.

The likelihood prediction for new landslides, with volume bigger than V_l’ and V_l’’, is a much more difficult task as the volume is a complex value to be estimated (Catani et al., 2016). The exceeding probability of landslide volume used by Tacconi Stefanelli et al. (2020) was reached thanks to the knowledge of the alpha exponent of the statistical frequency distribution of the landslide volumes in the whole study area. To achieve this, a database of landslides with a very high number of events (tens or even hundreds of thousands) should be available (Catani et al., 2016), which in our study area unfortunately is not. To have an assessment of the damming susceptibility for neo-formed landslides the two volume threshold values, evaluated for all the river networks, can be used as well. After estimating the river width of every river stretches, the V_l’ and V_l’’ values of each of them can be computed through the corresponding two equations. In this way there will be two reference values to be able to assess whether the volume of a new landslide can potentially obstruct an affected river stretch.

The input data needed for the procedure are a Digital Elevation Model, a vector layer of the river network, and an updated landslide inventory. The data quality and resolution such as the landslides inventory completeness, the river network reliability and the DEM’s pixel size heavily affect the quality of the result (Tacconi Stefanelli et al., 2020). Thus, it was decided to use the DEM with the higher resolution freely available from the NASA’s SRTM project (Far and Kobrick, 2000) with a 1 arc-second, or about 30 meters of resolution. The river network came from Coccia et al. (2023). The latter input data is a database of 8910 landslides, that is a compilation of several different inventories collected through decades of field surveys, studies and remote sensing analysis in the study area, shown in Figure 4.

Hereafter the detail of each inventory:

- The “Rockslides and Rock Avalanches of Central Asia” (Strom and Abdrakhmatov, 2018): an inventory including more than 1000 of very big (>=1 Mm^3) rockslides and rock avalanches, covering central Asian countries (excluding Turkmenistan and Altai) and also Chinese Tien Shan and Pamir, and Afghan Badakhshan. Collected in decades of field survey and analysis of aerial/satellite imaging, it includes also information on morphometric parameters (runout, area), dammed lakes, head-scarps, and quantitative characteristics (such as area, volume) for about 600 cases.

- The “Tien Shan landslide inventory” (Havenith et al., 2015a): is the biggest database in the study area. Assembled through field work, remote sensing and geophysical data interpretation, it includes the elements of the previous inventory alongside other smaller landslides in soft sediments (Havenith et al. 2006a; Schlögel et al., 2011) for a total of 3,462 landslides polygons, including information on landslide length and area.

- The “Multi-temporal landslide inventory for a study area in Southern Kyrgyz Republic derived from RapidEye satellite time series data (2009 – 2013)” (Behling et al., 2014; 2016; Behling and Roessner, 2020), includes 1,582 landslide polygons mapped from multi-sensor optical satellite time series data (from 1986 to 2013) over an area of 2,500 km^2 in the Fergana valley rim in southern Kyrgyz Republic, and include information on landslide activity (area and year of trigger).

- The “Tajikistan landslide database” produced by the Institute of Water Problems, Hydropower, Engineering and Ecology of Tajikistan (IWPHE), with 2,710 landslide polygons and 114 landslide-prone areas, including information on landslides length and area.

- The Institute of Seismology of the Academy of Science of Uzbekistan (ISASUZ) provided an inventory which covers the Tashkent province composed by a point inventory (Niyazov, 2020) and a polygon inventory (345 landslide) digitized from the maps in Juliev et al., 2017.

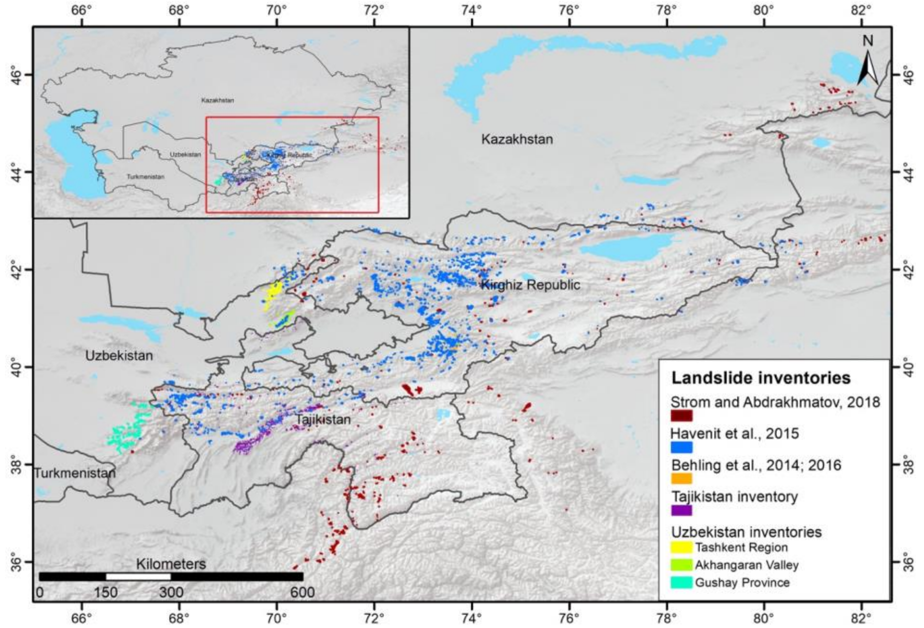

Figure 4. Map of the landslide inventories in the study area. Lake's polygons from Esri, Garmin International, Inc.; basemap from Esri, USGS, NOAA.

The methodology adopted to obtain the maps of damming susceptibility, derived from Tacconi Stefanelli et al. (2020), is summarized in the following main steps displayed in Figure 5. According to the literature (Swanson et al., 1986; Fan et al., 2014; 2020; 2021; Tacconi Stefanelli et al., 2015; 2018), river obstructions occur in most of the time within hilly or mountainous areas and specially along steep slopes. Therefore, considering the extension of the study area, in order to reduce the time of elaboration and improve the visualization of the results, in step I of Figure 5 a series of unnecessary data were removed from the calculations during some preliminary operations. For this reason, river that flow in flat areas (with less than 4° slopes) were not considered in the elaborations, since their damming probability is certainly very low with an extremely wide valley width. Additionally, to have maps easier to manage and display, the river network was split in 5 km long river stretches consecutive to each other.

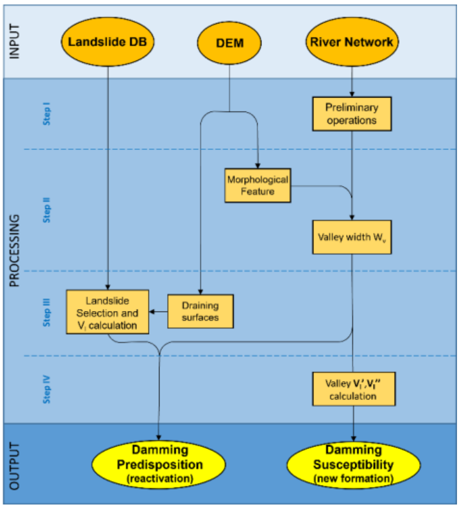

Figure 5. Flow chart of the main steps of the mapping methodology.

In applied geomorphology and natural science studies the analysis and characterization of the landscape has evolved during the last decades with the increasing accessibility of remote sensing data and the development of different algorithms able to automatically extract morphological features and landform information even at broad scales (Drăguţ and Dornik, 2016; Maxwell and Shobe, 2022; Righini and Surian, 2018; Wang et al., 2010).

As already mentioned, the clear definition of the width of a river can be subjective and its measurement difficult to repeat especially if performed by different operators. In step II of Figure 5, an objective automatic method to extract morphometrical parameters have been chosen also for this reason. Wood (2009) implemented the "*LandSerf*" software (already incorporated in SAGA GIS or QGIS software), designed to automatically classify landforms from DEMs. Similarly for pattern detection and texture analysis within image processing, the software extracts land-surface parameters (e.g., slope, aspect, and curvature) from DEMs through a multi-scale approach. During these processing, the algorithm performs a classification of the landscape, grouping the landforms with homogeneous morphometric characteristics (pits, channels, peaks, ridges, passes, and planes) as shown in Figure 6. Thanks to this algorithm of morphological forms analysis proposed by Wood (2009), the polygons representing the morphological unit of the river valley can be automatically defined objectively even in a large area and extracted.

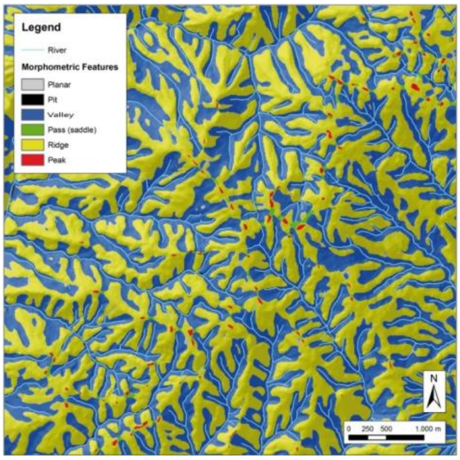

Figure 6. Classification of the landscape into morphological classes according to Wood (2009) (modified from Tacconi Stefanelli et al., 2020).

The effectiveness of distinguishing different morphological landforms of this automatic tool is greater in mountainous regions characterized by significant differences in elevation, compared to flat areas where distinctions between landforms are less evident. The accuracy of the output is directly correlated with the resolution of the DEM, which should ideally be about a few meters. Coarser resolutions result in landslide volumes with a corresponding level of uncertainty.

The following phase is to provide to each river stretch a value of a valley width, W_v. A series of 1 km long lines (hereafter "transects") are generated, perpendicular to the stretches of the river network, outdistanced by 500 meters apart from each other. The created river valley polygons are used to "cut" the transects and then to measure the distance between the two river valley borders through the length of the cut transects.

Next, the valley widths (W_v) for each segment of the river are determined by assigning them an average value based on N perpendicular transects, excluding the extreme values (maximum and minimum, respectively W_{max} and W_{min}), as in the fallowing equation:

$$W_v = \left(\sum_{i=1}^{n} W_i - W_{min} - W_{max}\right)\frac{1}{n-2} \tag{4}$$

By utilizing an updated database of landslide polygons, in the step III of Figure 5 it is possible to determine if a reactivated landslide is big enough to cause a complete river blockage thanks to the comparison with the boundary volumes of V_l' (below which a landslide cannot completely block the river) and V_l'' (above which the river valley is dammed for sure). A reactivated landslide should follow a downhill path akin to the flow of surface water. Within each slope, the drainage directions can be easily determined along the river network using a GIS software. Each mass movement can then be linked to the corresponding river stretch it would reach if reactivated based on their corresponding draining surfaces.

Since the information provided by the available inventories in the study area are not homogeneous and comparable, for the computation of the landslide volume were chose to use the areas of the landslide polygons, since it is the most common data. An experimental statistical relationship between areas and volumes was applied:

$$V_l = \varepsilon \cdot A_l^{\alpha} \qquad (5)$$

where V_l and A_l are respectively the volume and the area of a landslide, ε and α are respectively the constant and the exponent of the power law describing the landslides volumes frequency distribution. Various experimental relations of ε and α have been employed for landslide volume calculations by researchers located in different countries. After an evaluation of these relations in the study area, the parameter proposed by Guzzetti et al. (2009) have been selected because of the number of the studied cases (667) and the magnitude range of the landslides area investigated (from 10^1 to 10^9 m^2). The landslide volume computed using this procedure is based on some approximations, since they use geometric simplifications, but it does still reflect the magnitude of the process. The result of the computation in Figure 7 shows an almost bimodal distribution, in which most landslides (83%) have moderate volumes, lower than 10 million m^3 (with 63% lower than 1 million m^3), but 4% have value higher than 100 million m^3.

Then, Table 1~~Table 1~~ is used to assign to each landslide of the inventory a classification based on the comparison with the boundary volumes V_l' and V_l'', with value of 2 if the calculated landslide volume, V_l, is bigger than V_l' (or V_l''), of 0 if it is smaller. For more caution, the V_l values is increased by an arbitrary value of 20% ($V_l \cdot 1.2$) to avoid any potential underestimation during volume estimation and even the possible increase of landslide size with the reactivation due to the mechanism of material entrainment (Hungr and Evans, 2004). For each landslide, if the computed boundary volume V_l' (or V_l'') is bigger than the estimated landslide volume V_l, but smaller than $V_l \cdot 1.2$, then a classification value of 1 is attributed.

The damming susceptibility of each mapped landslide is assigned by integrating the two comparative classification values from the intensity matrix illustrated in Figure 8. The matrix establishes five qualitative classes on a scale of severity for damming susceptibility, ranging from Very Low (dark green) to Low (light green), Moderate (yellow), High (orange), and Very High (red). The combination of a high V_l" value (1 or 2) and a lower V_l' value (0 or 1) symbolized by gray squares is not possible according to their respective formulations.

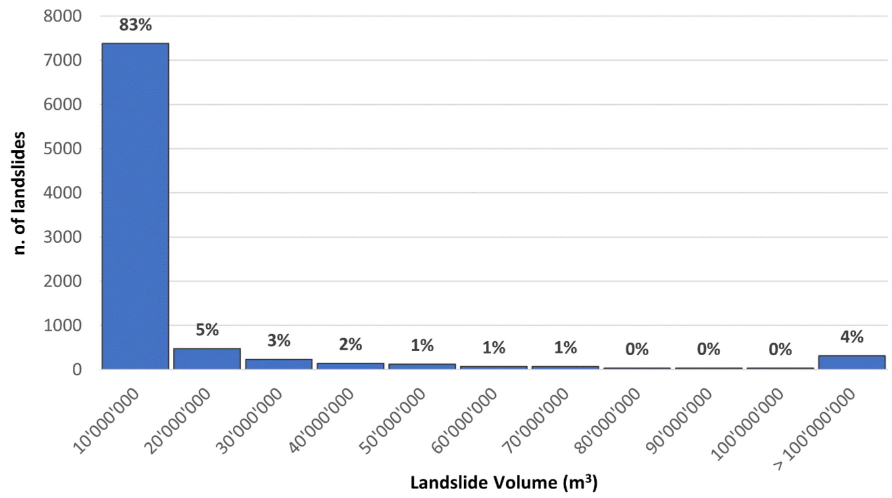

Figure 7. Landslide volumes frequency distribution in the central Asia regions.

Table 1. Comparison table between landslide calculated volumes, V_l, with the boundary volume of Non-formation and Formation, V_l' and V_l''(after Tacconi Stefanelli et al., 2020).

	$V_l > V_l'$ (V_l'')	$V_l < V_l'$ (V_l'') $< V_l * 1.2$	$V_l < V_l'$ (V_l'')
Classification Value	2	1	0

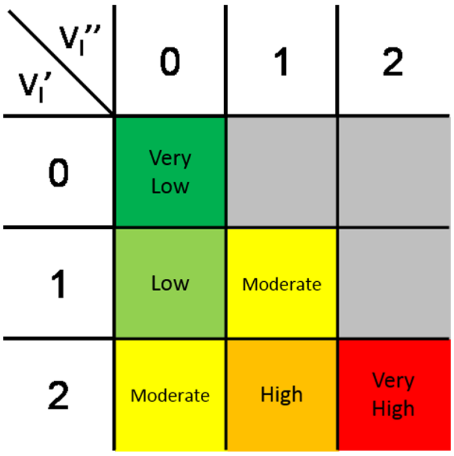

V_l' \ V_l''	0	1	2
0	Very Low		
1	Low	Moderate	
2	Moderate	High	Very High

Figure 8. Predisposition matrix used for the assignment of the damming predisposition intensity to the mapped landslides (after Tacconi Stefanelli et al., 2020).

Even if the proposed method is objective, it is certainly not free from uncertainties and errors. The 20% increase applied to mapped landslide volumes to reduce underestimation errors can in turn produce false positives for overestimation errors. While a false positive is preferable to a false negative (according to a principle of prudence), too many high-risk false positive cases "spread" an unreal risk throughout the area instead of concentrating it in sites of real risk. Therefore, it can be assumed that the landslide bodies which have previously reached the valley floor have already generated most of their effect on the river network (Strom, 2010) or have had no effect, spending their potential risk component. These landslides, also with a volume higher than V_l' and V_l'' and therefore classified with Very High dam predisposition, even if reactivated probably will not produce any further effect in the future. For these reasons, it was decided to downgrade the classification of those landslides that intersect the river network by reducing its position of the classification of damming predisposition by one class.

Using the W_v value for each river stretches estimated during the step III of Figure 5, in the last step (IV) the two boundary landslide volumes, namely "Non-formation volume" and "Formation volume" (V_l' and V_l''), can be estimated by applying the equations of the "Non-formation" (Eq. (2)) and "Formation" lines (Eq. (3)). These two values can be used both to classify the damming susceptibility of the river network (for new landslides) and of the landslides inventory (for their reactivation). For the first case, the computed volume values V_l' and V_l'' embody the required volumes of a new landslide to have a potential or certain (with 99% of confidence) obstruction for each river stretches.

4 Results

The mapping methodology was applied to all the studied territories of the Central Asia region in order to analyze and evaluate the results. Two smaller basins, the upper Pskem river and the Fergana valley, were selected to verify the reliability at a catchment scale of the results obtained from a methodology applied on a national scale. The assessment of damming predisposition on the available landslide inventory on the Central Asia regions is shown in the map of Figure 9, while a closer detail is reported in ~~Figure 11~~ Figure 10 showing the Kyrgyz Republic territory. The number of landslides (644 cases) classified with Very High damming predisposition from the whole inventory before the class reduction due to the river intersection was unjustifiably and unreasonably large posing excessive concern and risk perception. After the change, this number decreased by 75% up to 166 cases, a high number but more reasonable concerning such a large area. In the class distribution of the damming predisposition ~~shown in Figure 10~~ the most frequent class is the Very Low, with 81% of the whole database, followed by the Low and High classes both with 6% and the remaining percentage divided among Moderate (5%) and Very High (2%).

This distribution is quite coherent with the landslide volumes frequency distribution since it is reasonable to associate landslides with very low volume (83%, shown in Figure 7) with those classified with very low susceptibility (81%~~, Figure 10~~). The landslides classified with the higher values of susceptibility (Moderate, High, and Very High with a total of 13%) instead do not only include landslides with higher volumes (more than 100 million m^3 representing 4% of the total), meaning that also even smaller landslides can potentially block narrow river stretches in these regions.

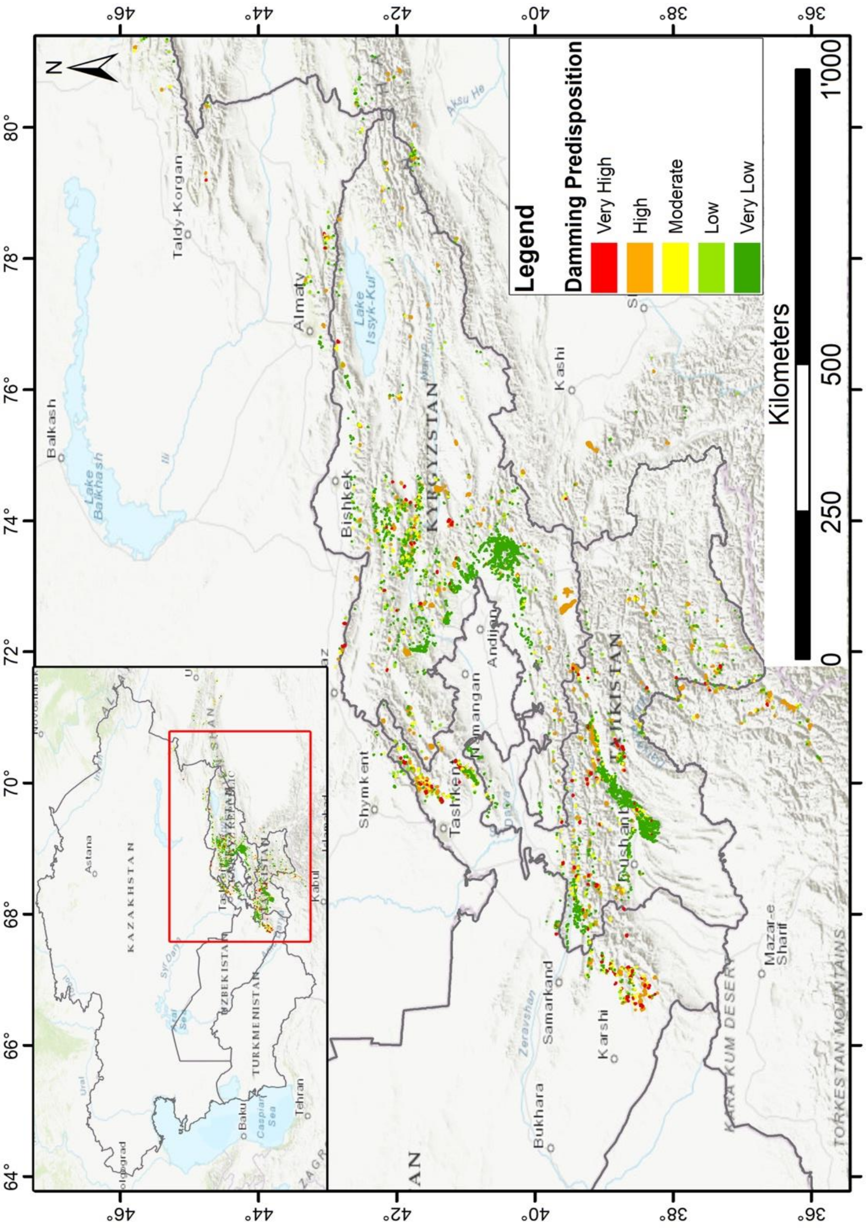

Figure 9. Map of Central Asia Landslide Damming Susceptibility. Basemap source: Esri, HERE, Garmin Intermap, increment P Corp, GEBCO, USGS, FAO, NPS, NRCAN, GeoBase, IGN, Kadaster NL, Ordnance

Survey, Esri Japan, METI, Esri China (Honk Kong), © OpenStreetMap contributors, and the GIS User Community.

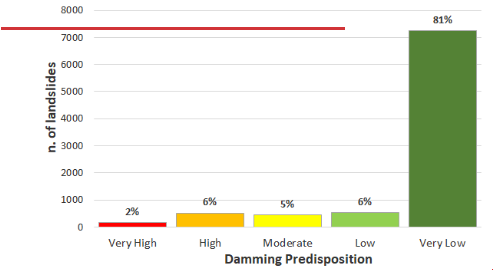

~~Figure 10. Classes distribution of the damming predisposition for landslides reactivation.~~

Formattato: Mantieni con il successivo

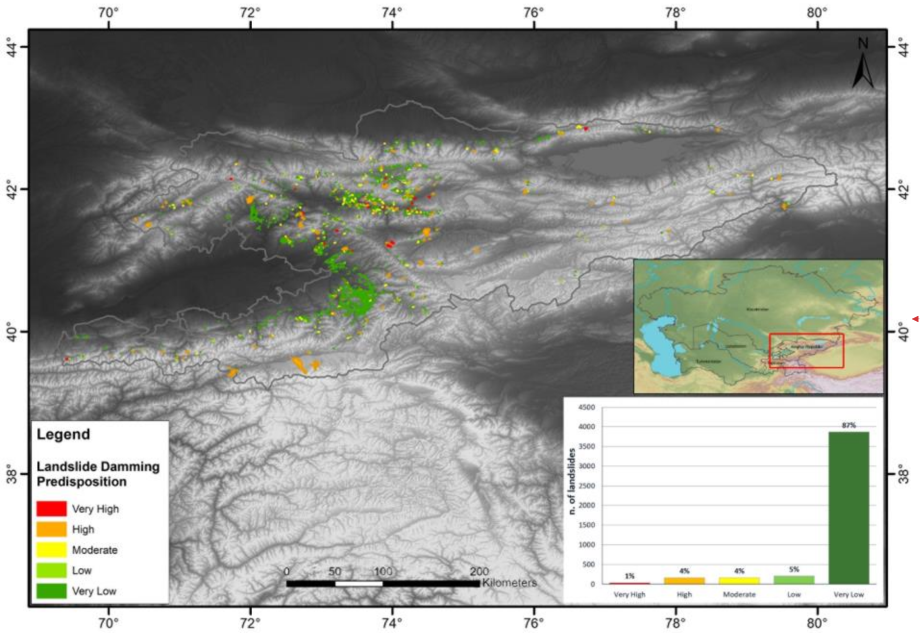

Figure 10. Map of Damming Predisposition by landslides reactivation in Kyrgyz Republic territory.

~~Figure 11. Map of Damming Predisposition by landslides reactivation in Kyrgyz Republic territory.~~ Topographic base from NASA's SRTM project (Farr and Kobrick, 2000).

Concerning the damming susceptibility caused by new landslides along all the river network in the study area, two different maps of the river networks have been produced using the Non-formation and Formation volumes values.

Although counterintuitive at first glance, these maps provide complementary information. The former provides the volumes of landslides that surely create an obstruction, while the latter the volumes below which it definitely does not form. According to the preliminary steps of the described methodology, in the river stretches running in flat areas (slope degree less than 4° representing the 88.4% of the entire river network) the analysis has been not applied, due to the extreme unlikelihood that a complete obstruction will occur in such areas. The magnitude of the damming susceptibility of the river networks has been classified in five classes and shown in ~~Figure 12~~ Figure 11 and ~~Figure 15~~ Figure 13. The five volumes intervals describing damming susceptibility were decided according to general value distribution of landslides volumes and an expert judgement. Since small landslides are more frequent than large ones, as reported in Figure 7, the lower is the landslide volume required to realize an obstruction, the higher is the magnitude. In the map of damming susceptibility related to the "Non formation", reported in ~~Figure 12~~ Figure 11, 88.4% of the regional river network lies in lowlands areas while ~~the central classes,~~ Moderate and Low classes are the most frequent with 4.4% and 5.8% respectively~~, as reported in Figure 13~~. This means that in most of the river stretches in the study area the minimum landslide volume able to potentially dam the riverbed is between the limit values of the two classes, from 2,5 to 25 million m^3. The following most frequent class is the Very Low with 0.8% and only a very small portion of the river stretches are classified as High and Very High with just 0.4% and 0.2% with a required landslide volume less than 2.5 million m^3. An example of close-up on the Tajikistan territory is reported in ~~Figure 14~~ Figure 12.

Regarding the map of damming susceptibility related to Formation values, the map in Figure 13~~Figure 15~~ shows slightly different results. The most frequent classes are the two lower ones, Low and Very Low with 4.4% and 6% respectively~~, as described in Figure 16~~. Only just the 0.3% and 0.4% fall in the classes Very High and High damming susceptibility. A close-up on the Kyrgyz Republic is reported in ~~Figure 17~~ Figure 14.

The results of the classification for the river networks of each state are shown in Figure 15~~Figure 18 to Figure 22~~. The landslides of Tajikistan, Kyrgyz Republic, Uzbekistan and Kazakhstan regions have been classified according to damming predisposition (~~Figure 18~~Figure 15-a., Figure 15-d., Figure 15-g. and Figure 15-j.~~Figure 19-a., Figure 20-a. and Figure 21-a~~). In the Turkmenistan territory, it was not possible to assess any damming predisposition by landslides reactivation since the absence of any available landslide inventory. The results of Uzbekistan and Kazakhstan regions (Figure 15-g. and Figure 15-j.~~Figure 20-a. and Figure 21-a.~~) are a bit different from Kyrgyz Republic and Tajikistan regions due to the different availability of landslide inventories and a different orographic and valleys morphology of the formers national territories. As already mentioned, for a clearer comprehension of the damming susceptibility classification of the river network at the national level, the river stretches flowing in lowlands have not been considered in the analysis. Concerning the Damming Susceptibility of Non-Formation (Figure 15~~Figure 18~~-b., Figure 15-e., Figure 15-h., Figure 15-k. and Figure 15-m.~~Figure 19-b., Figure 20-b., Figure 21-b. and Figure 22-a.~~), the most frequent are Low and Moderate classes, followed by Very Low class. Fortunately, only very few river stretches have been classified as Very High and High. For the Damming Susceptibility of Formation (Figure 15~~Figure 18~~-c., Figure 15-f., Figure 15-i., Figure 15-l. and Figure 15-n.~~Figure 19-c., Figure 20-c., Figure 21-c. and Figure 22-b.~~) most of the rivers fall into Very Low and Low classes, followed by Moderate class. Also in this case, only very few river stretches have been classified as Very High and High. The results of the Tajikistan territory are quite similar to the Kyrgyz Republic and Uzbekistan with which it shares a similar orographic distribution and morphology of the territory. Turkmenistan and Kazakhstan show a slightly different distribution with higher percentage on Moderate class in the Damming Susceptibility of Non-Formation and Low class in the damming susceptibility of Formation.

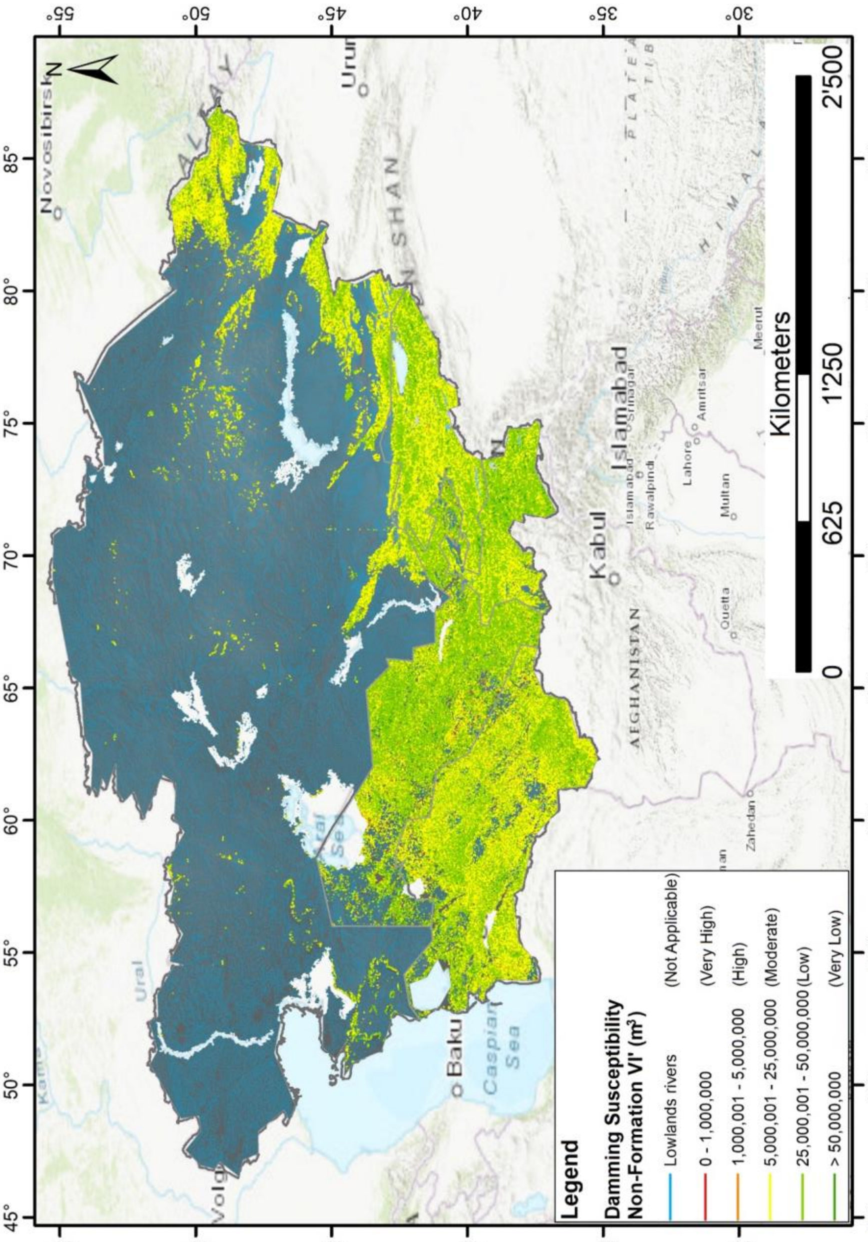

Figure 11. Damming susceptibility map of non-formation of river stretches by new landslides in the region.

Formattato: Mantieni con il successivo

Formattato: Didascalia;Figure caption;Légende italique, Giustificato

~~Figure 12. Damming susceptibility map of non-formation of river stretches by new landslides in the region.~~ River network database from Coccia et al.~~,~~ (2023). Basemap source: Esri, HERE, Garmin Intermap, increment P Corp, GEBCO, USGS, FAO, NPS, NRCAN, GeoBase, IGN, Kadaster NL, Ordnance Survey, Esri Japan, METI, Esri China (Honk Kong), © OpenStreetMap contributors, and the GIS User Community.

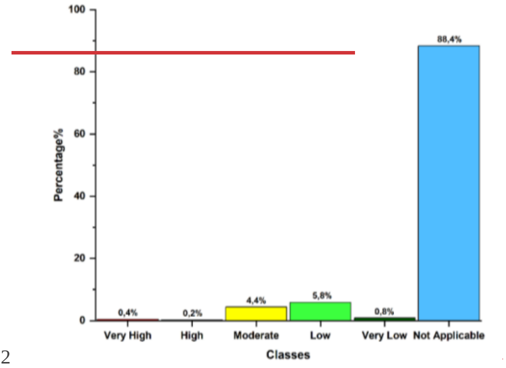

~~Figure 13. Distribution of the damming susceptibility in the study area by new landslides related to Non formation boundary values.~~

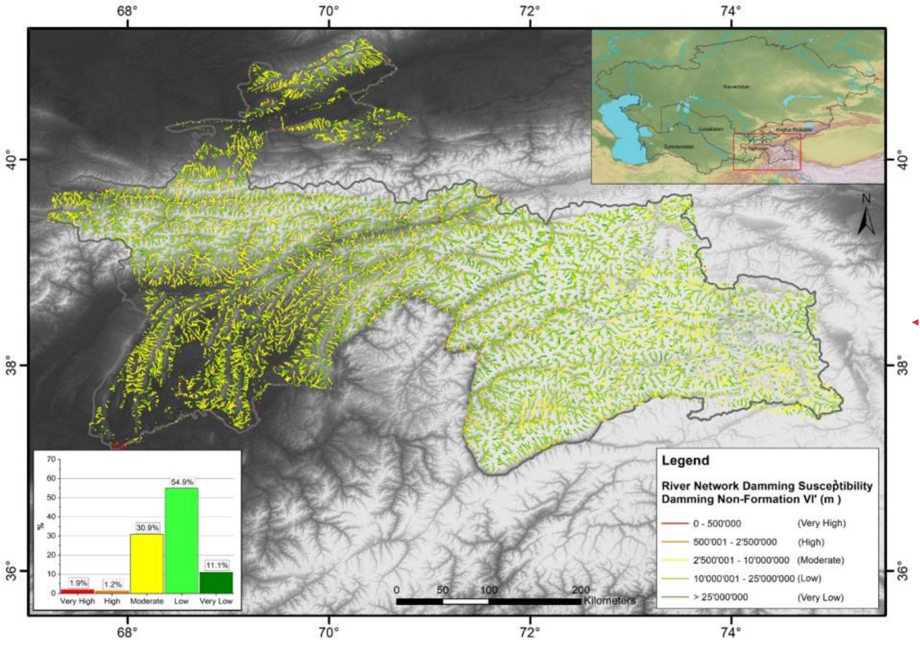

Figure 12. Damming Susceptibility Map of non-formation of river stretches by new landslides in Tajikistan.

Formattato: Mantieni con il successivo

Formattato: Didascalia;Figure caption;Légende italique, Giustificato

~~**Figure 14. Damming Susceptibility Map of non-formation of river stretches by new landslides in Tajikistan.**~~ River network database from Coccia et al.~~,~~ (2023). Topographic base from NASA’s SRTM project (Farr and Kobrick, 2000).

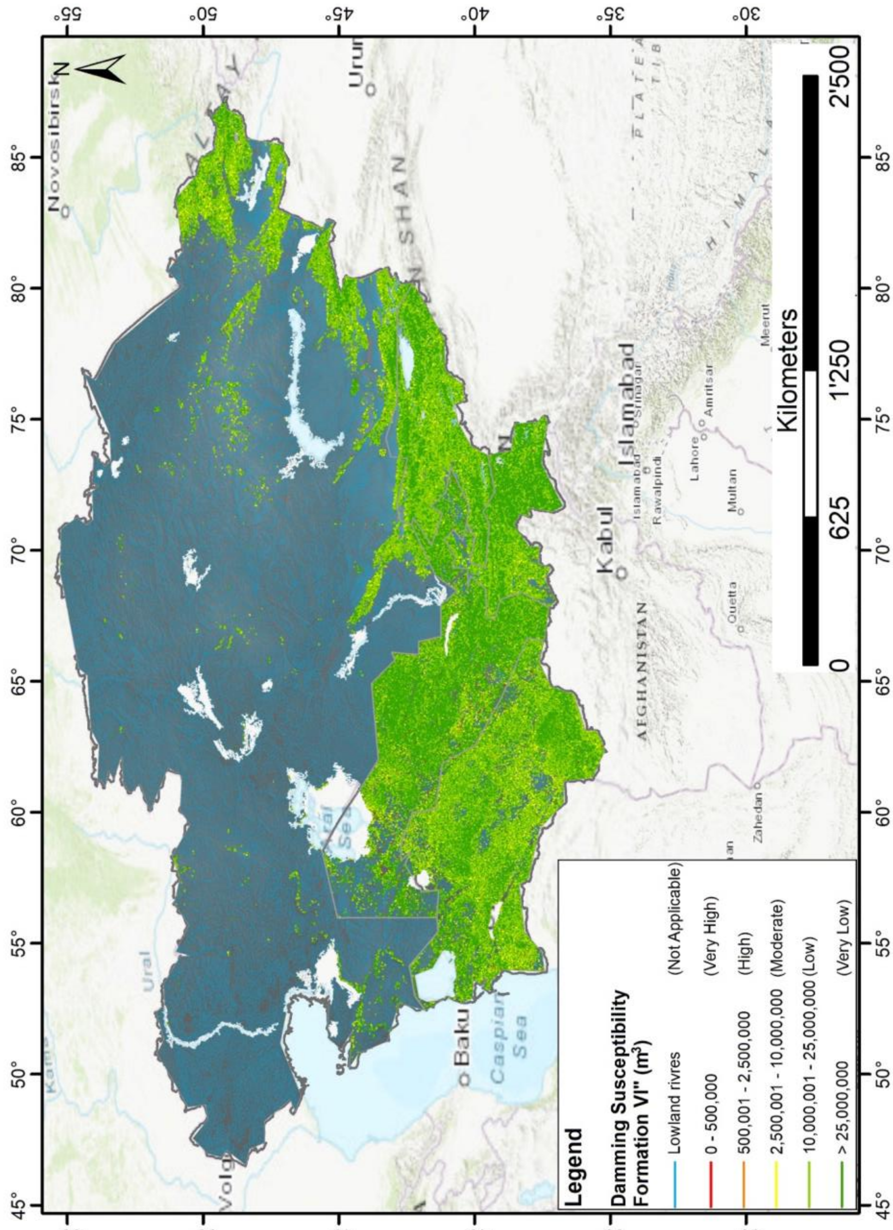

Formattato: Mantieni con il successivo

Figure 13. Damming Susceptibility Map of Formation of river stretches by new landslides in the region

Formattato: Didascalia;Figure caption;Légende italique, Giustificato

~~Figure 15. Damming Susceptibility Map of Formation of river stretches by new landslides in the region~~. River network database from Coccia et al.~~,~~ (2023). Basemap source: Esri, HERE, Garmin Intermap, increment P Corp, GEBCO, USGS, FAO, NPS, NRCAN, GeoBase, IGN, Kadaster NL, Ordnance Survey, Esri Japan, METI, Esri China (Honk Kong), © OpenStreetMap contributors, and the GIS User Community.

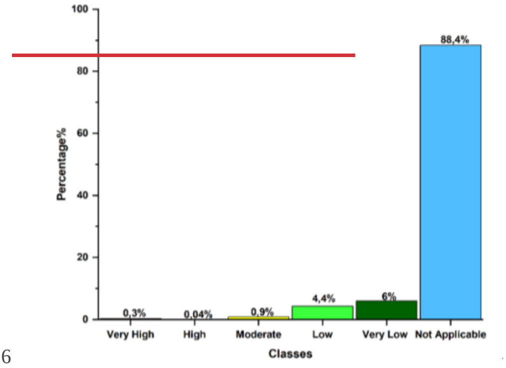

~~Figure 16. Distribution of the Damming Susceptibility in the study area by new landslides related to Formation boundary values.~~

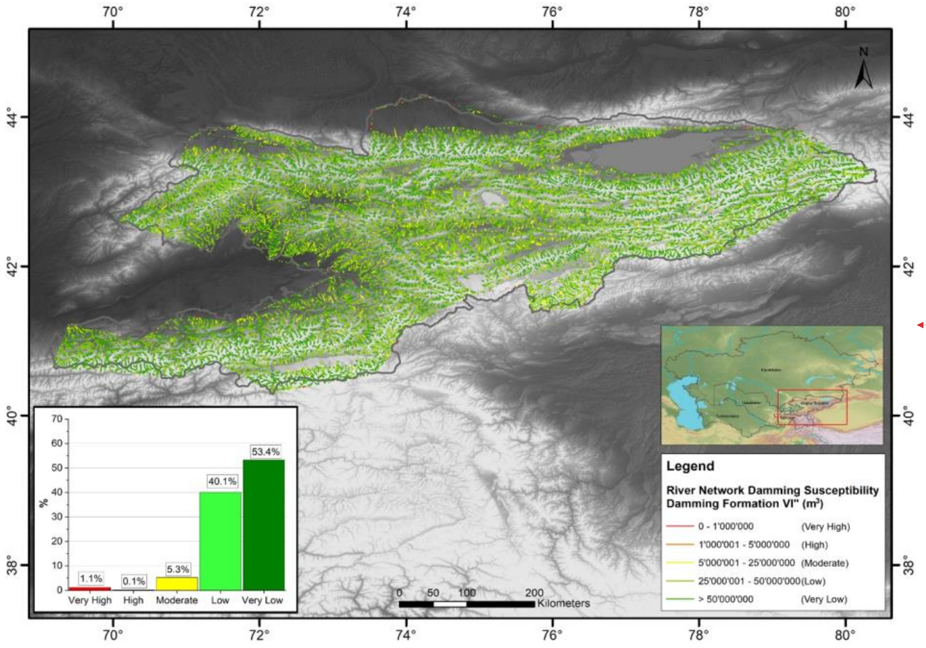

Formattato: Mantieni con il successivo

Figure 14. Damming Susceptibility Map of formation of river stretches by new landslides in the Kyrgyz Republic territory

Formattato: Didascalia;Figure caption;Légende italique, Giustificato

~~Figure 17. Damming Susceptibility Map of formation of river stretches by new landslides in the Kyrgyz Republic territory~~. River network database from Coccia et al.~~,~~ (2023). Topographic base from NASA's SRTM project (Farr and Kobrick, 2000).

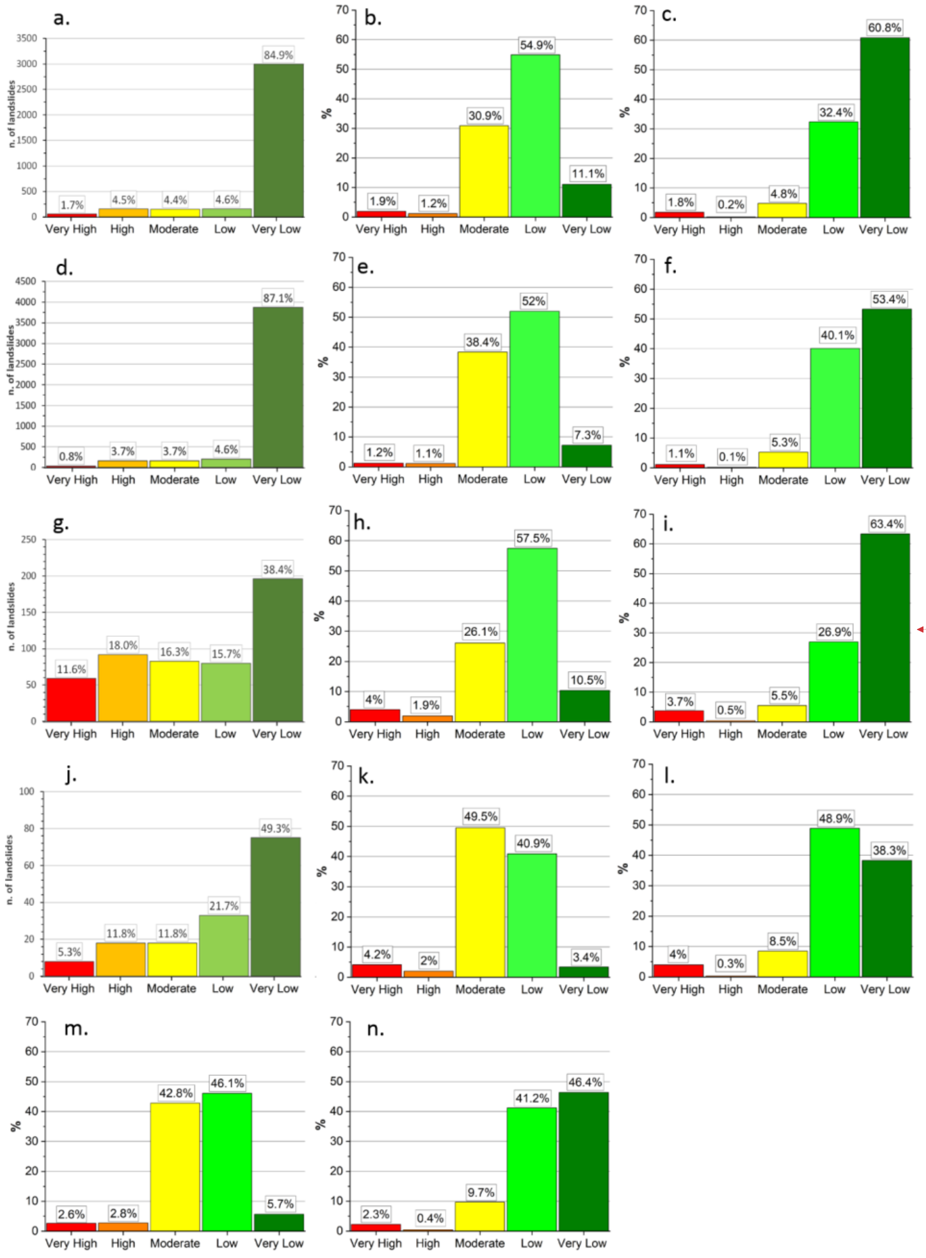

Figure 15. Classes distribution of Damming Predisposition for landslides reactivation, Damming Susceptibility of Non-Formation and Formation for new landslides

Formattato: Mantieni con il successivo

~~Figure 18. Classes distribution in Tajikistan of the Damming Predisposition for landslides reactivation (a.), Damming Susceptibility of Non-Formation (b.) and of Formation (c.) for new landslides~~, in Tajikistan (a.), (b.) and (c.), in Kyrgyz (d.), (e.) and (f.), in Uzbekistan (g.), (h.) and (i.), in Kazakhstan (j.), (k.) and (l.), in Turkmenistan (m.) and (n.).

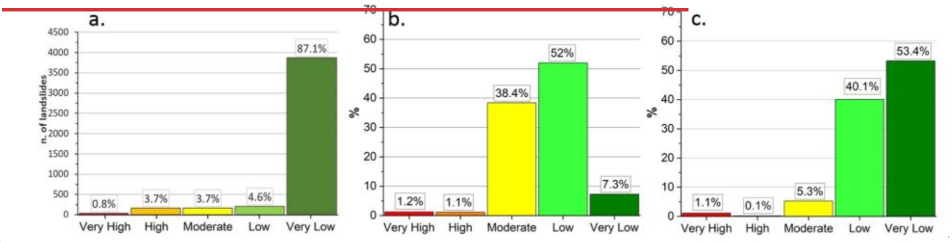

~~Figure 19. Classes distribution in the Kyrgyz Republic of the Damming Predisposition for landslides reactivation (a.), Damming Susceptibility of Non-Formation (b.) and of Formation (c.) for new landslides.~~

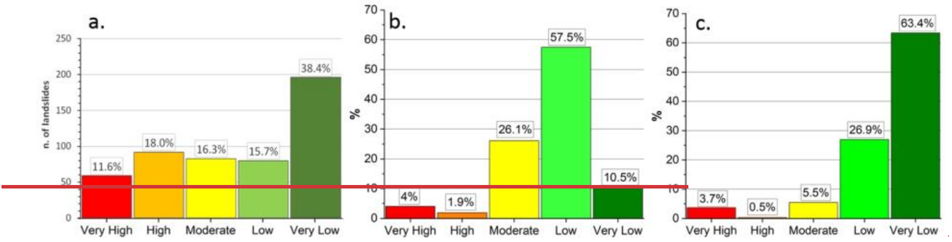

~~Figure 20. Classes distribution in Uzbekistan of the Damming Predisposition for landslides reactivation (a.), Damming Susceptibility of Non-Formation (b.) and of Formation (c.) for new landslides.~~

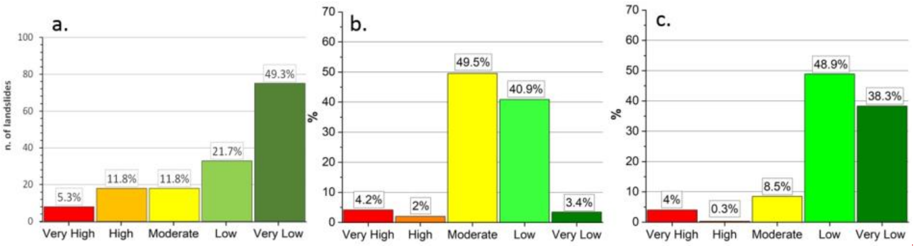

~~Figure 21. Classes distribution in Kazakhstan of the Damming Predisposition for landslides reactivation (a.), Damming Susceptibility of Non-Formation (b.) and of Formation (c.) for new landslides.~~

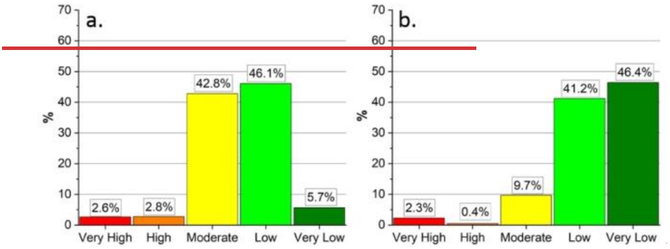

~~**Figure 22. Classes distribution in Turkmenistan of the Damming Susceptibility of Non-Formation (a.) and of Formation (b.) for new landslides.**~~

~~4.9~~4.1 Upper Pskem river valley (Uzbekistan)

The Pskem river, locate in the Tashkent region of Uzbekistan, is a right-hand tributary of the Chirchik River that is the feeder of the Syr Darya river basin (in the Western Tien-Shan). The river originates from the confluence of the Maidantal and Oygaing rivers and is one of the main tributaries of the Charvak Lake (Semakova et al., 2016). This artificial lake is central for the local economy for its functions as reserve for fishing and water, as well as a source of hydroelectric energy and because of that various villages arise around it and downstream. The formation of a natural obstruction and an upstream impoundment in the Pskem basin could be a serious threat due to the possible instability of the earth dam and for the possible catastrophic cascade effects that its collapse could have downstream on the artificial basins and their 168 meters high earthfill dam.

With a careful observation of the map of Damming Predisposition by landslides reactivation in the lower Pskem basin in an area of 443 km^2 (Figure 16~~Figure 23~~), some of the 53 mapped landslides should be subjected to further study. Among all, most landslides were classified with a Very Low and Low predisposition value, respectively 21 and 11 cases (39.6% and 20.8%), and only 4 landslides with a Very High value (7.5%), 10 with High (18.9%) and 7 with Moderate (13.2%). Landslides named A, B, C, D and E in~~ Figure 23~~ Figure 16, if reactivated will potentially cause an obstruction of the main river section of the Pskem, being classified the first three and the latest two respectively with High and Very High damming predisposition. As shown in Table 2, the volumes of all these landslides are way bigger than the boundary volume of Non-Formation and Formation from ~~Figure 24~~ Figure 17 and~~ Figure 25~~ Figure 18. It is important to notice that the landslides A, B and C are laid down in the valley floor, meaning that in the past they had probably already dammed the river in that point, and the classification of their damming predisposition have been reduced by one, from Very High to High. Due to the considerable volumes of the landslides in the basin and the presence of landslides that have probably already blocked the river in the past, this relatively small area is certainly worthy of attention.

Table 2. Landslides volumes and damming parameters W_v, V_l', V_l" of the landslides in Figure 16 ~~Figure 20~~ computed using the described method.

Landslide	V_l ~~-~~– Landslide volume (m^3)	W_v – River Width (m)	V_l' ~~-~~– Volume of Non-formation (m^3)	V_l" ~~-~~– Volume of Formation (m^3)
A	200.000.000	300	2.600.000	16.200.000

B	12.000.000	235	1.500.000	10.000.000
C	34.000.000	318	3.000.000	18.200.000
D	73.000.000	513	10.100.000	47.400.000
E	61.000.000	575	13.500.000	60.000.000

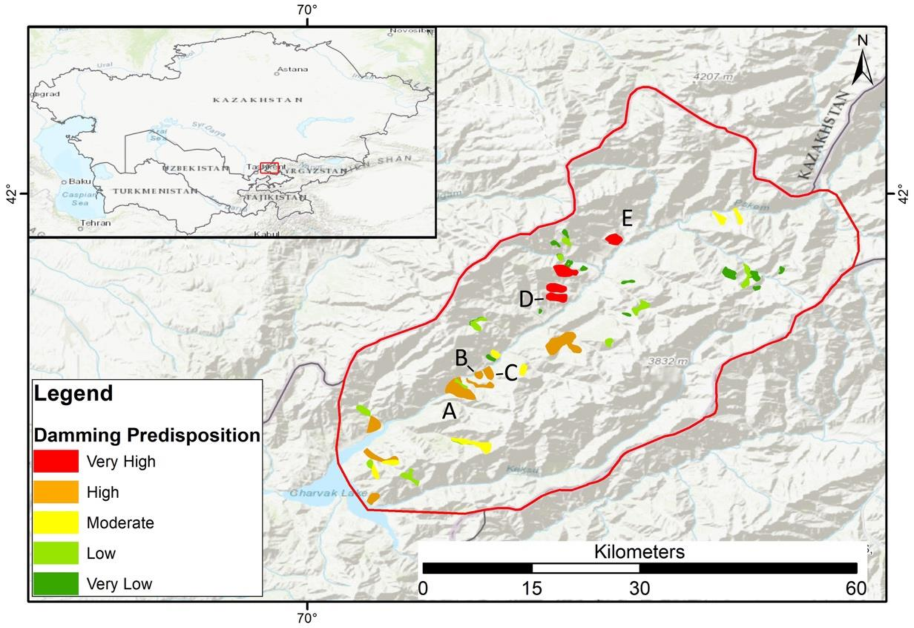

Figure 16.

~~Figure 23.~~ **Map of Damming Predisposition by landslides reactivation in the lower Pskem basin.** Basemap source: Esri, HERE, Garmin Intermap, increment P Corp, GEBCO, USGS, FAO, NPS, NRCAN, GeoBase, IGN, Kadaster NL, Ordnance Survey, Esri Japan, METI, Esri China (Honk Kong), © OpenStreetMap contributors, and the GIS User Community.

Formattato: Didascalia;Figure caption;Légende italique, Giustificato

The obstruction of the Pskem river by one of these landslides would cause an upstream impoundment with a surface from 2 to 10 km^2 or more, depending on the dam position and height. The dam collapse could release a catastrophic flooding wave with destructive effects in the downstream areas. In the worst scenario, even the earthfill dam located few kilometers downstream could be seriously damaged with unpredictable effects. Since the reliability of this mapping method is strictly correlated to the quality of the input data, when the used DEM has a coarse resolution, in similar cases of possible risk to people’s life it is always advisable to do a second "manual check" even using some free satellite imaging services like Google Earth. In fact, when the DEM resolution is too rough, the GIS tool used in this methodology to evaluate the extension of the riverbed morphologic unit can produce inconsistent and incorrect results, causing improper damming susceptibility evaluations. The results of the measurements on Google Earth orthophotos in Table 3 show that the difference between the river width values calculated with the mapping method (W_v) and those measured on Google Earth (W_{vGE}) can in some cases be substantial modifying the calculated boundary volumes V' and V'', although in this case they do not modify drastically the final classification of the five landslides.

The river network of the upper Pskem valley have been also classified producing the maps of Damming Susceptibility of Non-formation and Formation (Figure 17~~Figure 24~~ and ~~Figure 25~~ Figure 18 respectively). Concerning the Damming Susceptibility Map of Non-formation (~~Figure 24~~Figure 17), the most frequent are Low and Moderate classes with 65.1% and 22.6% respectively, followed by Very Low class with 11.1%. Only just 1.3% have been classified as High and 0.0% as Very High. For the Damming Susceptibility Map of Formation (~~Figure 25~~Figure 18) most of the rivers fall into Very Low and Low classes with 69.8% and 27.7%, followed by Moderate class with 2.1%. Only 0.4% have been classified as High and 0.0% as Very High.

Table 3. Damming parameters W_{vGE}, $V_l'_{GE}$, $V_l''_{GE}$ of the landslides in ~~Figure 23~~ Figure 16 computed with Google Earth observation.

Landslide	W_{vGE} – River Width (m)	$V_l'_{GE}$ - Volume of non-formation (m^3)	$V_l''_{GE}$ - Volume of Formation (m^3)
A	415	6.000.000	31.000.000
B	310	2.800.000	17.300.000
C	260	1.800.000	12.100.000
D	530	11.000.000	50.000.000
E	450	7.300.000	36.500.000

The general damming susceptibility of the valley is low but a singular river stretch, marked by a black circle in ~~Figure 24~~ Figure 17 and ~~Figure 25~~ Figure 18, classified with High susceptibility in both maps should be carefully evaluated. This river part is clearly noticeable in the middle of the area along the main river path, a bit upstream from the landslides named B and C. The high classification values mean that geographically in that point the valley width undergoes a shrinkage and for this reason even a relatively small landslide generated from the surrounding slopes can create an obstruction, therefore it would be worthy of a more detailed investigation.

Formattato: Mantieni con il successivo

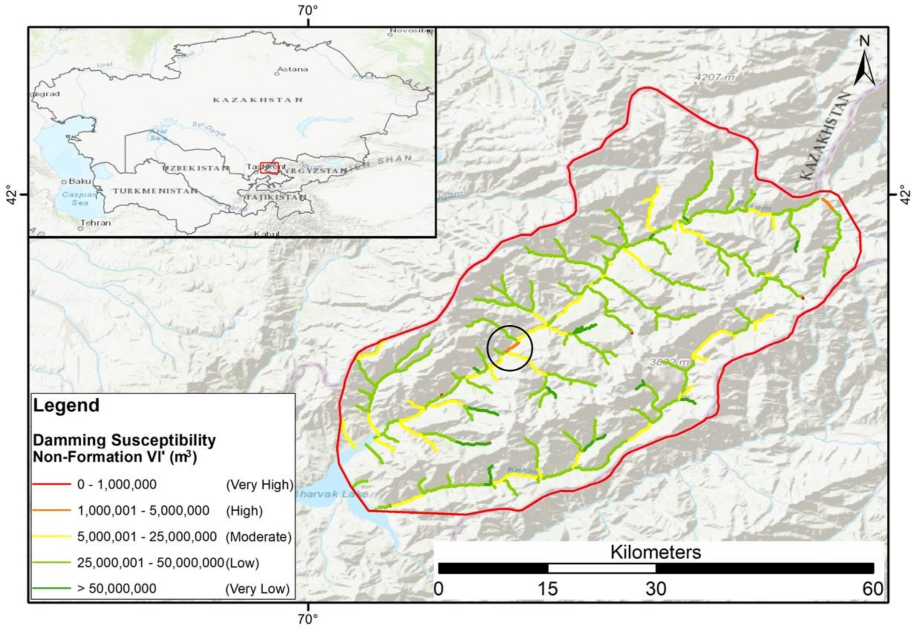

Figure 17. Damming Susceptibility Map of Non-formation of river stretches by new landslides in the lower Pskem basin. The black circle highlights a river stretch with unusually high values.

Formattato: Didascalia;Figure caption;Légende italique, Giustificato

~~**Figure 24. Damming Susceptibility Map of Non-formation of river stretches by new landslides in the lower Pskem basin. The black circle highlights a river stretch with unusually high values.**~~ River network database from Coccia et al.~~,~~ (2023). Basemap source: Esri, HERE, Garmin Intermap, increment P Corp, GEBCO, USGS, FAO, NPS, NRCAN, GeoBase, IGN, Kadaster NL, Ordnance Survey, Esri Japan, METI, Esri China (Honk Kong), © OpenStreetMap contributors, and the GIS User Community.

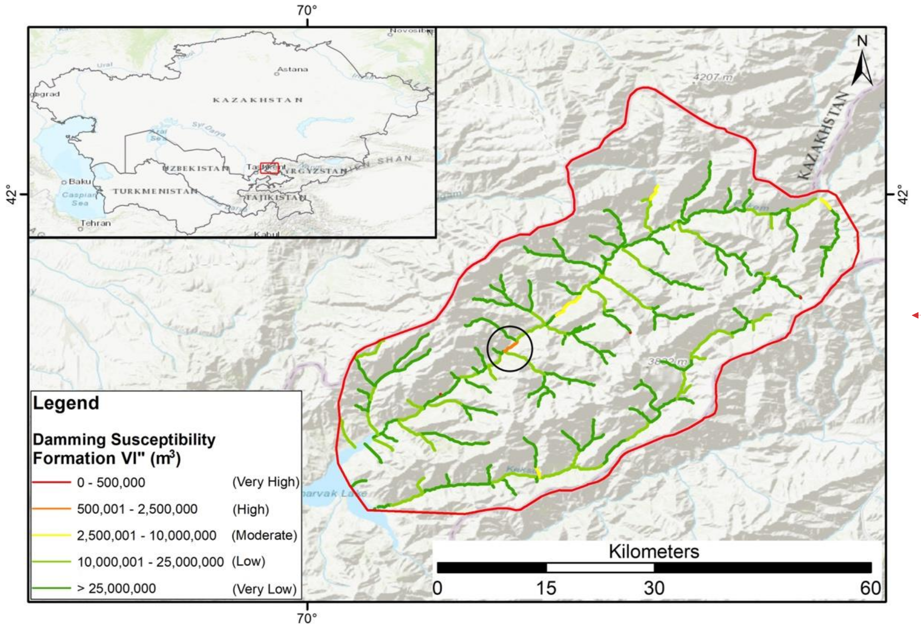

Figure 18. Damming Susceptibility Map of Formation of river stretches by new landslides in the lower Pskem basin. The black circle highlights a river stretch with unusually high values.

~~**Figure 25. Damming Susceptibility Map of Formation of river stretches by new landslides in the lower Pskem basin. The black circle highlights a river stretch with unusually high values.**~~ River network database from Coccia et al.~~,~~ (2023). Basemap source: Esri, HERE, Garmin Intermap, increment P Corp, GEBCO, USGS, FAO, NPS, NRCAN, GeoBase, IGN, Kadaster NL, Ordnance Survey, Esri Japan, METI, Esri China (Honk Kong), © OpenStreetMap contributors, and the GIS User Community.

~~4.10~~4.2 The Fergana valley mountainous rim (Tajikistan-Kyrgyz Republic-Uzbekistan)

The Fergana valley is one of the largest intermountain depressions in Central Asia located between Uzbekistan, Kyrgyz Republic, and Tajikistan. It hosts two main rivers, the Naryn and the Kara Darya, which join together to form the Syr Darya. In this populated area landslide activity is recurrent, causing every year damage to infrastructure and loss of human life, and triggered by complex interactions between multiple factors such as tectonic, geological, morphological and meteorological (Danneels et al., 2008; Schlögel et al., 2011; Piroton et al., 2020). The mapping methodology have been applied also to the Fergana valley and a total of 3370 landslides, coming from various data sources, have been classified as shown in ~~Figure 26~~ Figure 19. Comparably to the classification result of the entire inventory (Figure 9) most of the cases (94%) have a Very Low damming predisposition, followed by Low and Moderate (with 2.5% and 1.8% respectively) as reported in Table 4~~Table 4~~. Just very few landslides fall into High and Very High classes (with 1.4% and 0.3% respectively). For the

Formattato: Mantieni con il successivo

Formattato: Didascalia;Figure caption;Légende italique, Giustificato

ha formattato: Inglese (Stati Uniti) classification of the river network of the Fergana valley, the maps of Damming Susceptibility of Non-formation and Formation have been produced (Figure 20~~Figure 27~~ and Figure 21~~Figure 28~~ respectively). As a method with a multi-scale approach, in such large areas, this damming susceptibility method is suitable to provide territorial planning suggestions rather than indications on single interventions at local scale. The overall damming predisposition of the Fergana valley is quite low, considering the presence of 3370 mapped landslides in total, even if there are few landslides (10) classified with Very High damming predisposition which should be studied with more attention through localized analysis of damming susceptibility to ensure that downstream areas are not at risk and therefore require a specific monitoring.

Table 4~~Table 4~~ have been reported the distribution of the percentages of the damming susceptibility classes of those river stretches that are not running in flat areas, since these lowland rivers represent 53.6% of the total. Concerning the Damming Susceptibility Map of non-formation of the remaining river stretches (~~Figure 27~~Figure 20), the most frequent are Low and Moderate classes with 53.4% and 36.2% respectively, followed by Very Low class with 7.0%. Only just 2.1% and 1.3% have been classified as Very High and High. For the Damming Susceptibility Map of Formation (~~Figure 28~~Figure 21) most of the rivers fall into Very Low and Low classes with 54.5% and 38.1%, followed by Moderate class with 5.2%. Only 1.9% and 0.2% have been classified as Very High and High respectively.

ha formattato: Inglese (Stati Uniti)

Table 4. Distribution of Damming Susceptibility classes on existing landslides (~~Figure 26~~Figure 19) and on the river stretches for non-formation (~~Figure 27~~Figure 20) and Formation of new landslides (~~Figure 28~~Figure 21).

Damming Susceptibility	Landslides		non-formation	Formation
	n.	%	%	%
Very High	10	0.3%	1.9	1.7
High	48	1.4%	1.2	0.2
Moderate	61	1.8%	7.0	5.3
Low	83	2.5%	53.2	38.8
Very Low	3168	94.0%	6.7	54.0

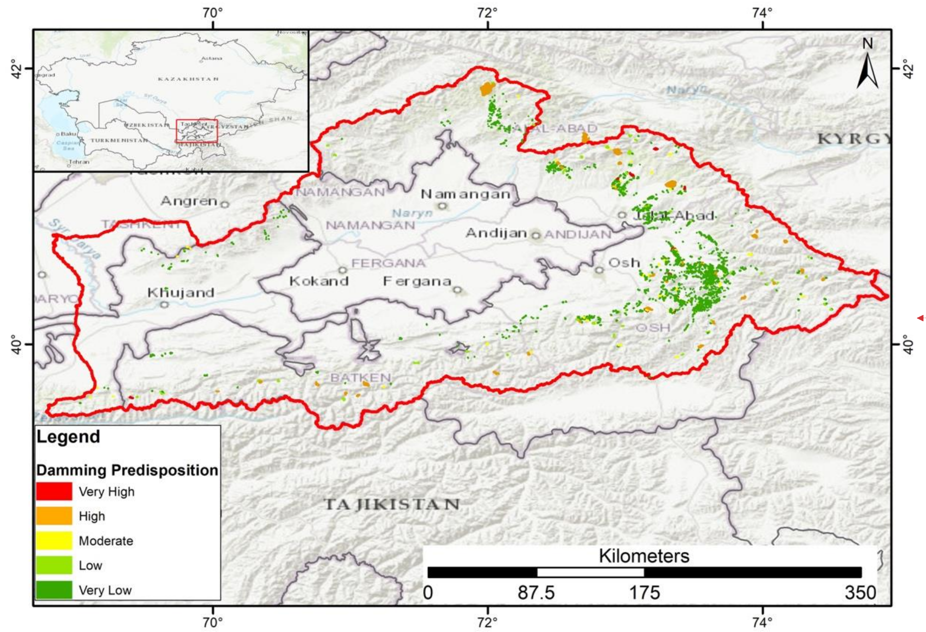

Figure 19. Map of Damming Predisposition by landslides reactivation in the Fergana valley

~~**Figure 26. Map of Damming Predisposition by landslides reactivation in the Fergana valley**~~. Basemap source: Esri, HERE, Garmin Intermap, increment P Corp, GEBCO, USGS, FAO, NPS, NRCAN, GeoBase, IGN, Kadaster NL, Ordnance Survey, Esri Japan, METI, Esri China (Honk Kong), © OpenStreetMap contributors, and the GIS User Community.

Formattato: Mantieni con il successivo

Formattato: Didascalia;Figure caption;Légende italique, Giustificato

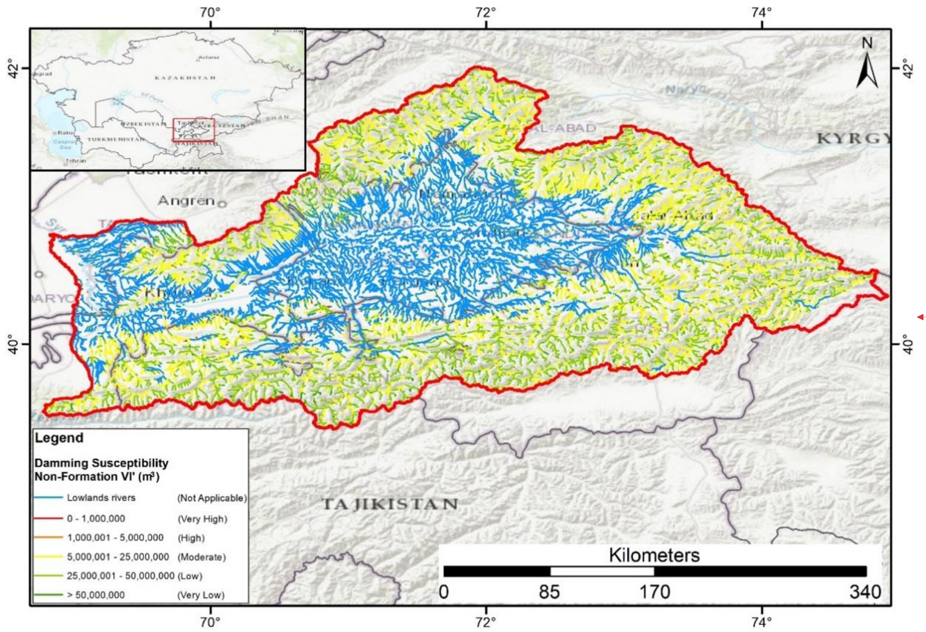

Figure 20. Damming Susceptibility Map of Non-formation of river stretches by new landslides in the Fergana valley

~~**Figure 27. Damming Susceptibility Map of Non-formation of river stretches by new landslides in the Fergana valley**~~**.** River network database from Coccia et al.~~,~~ (2023). Basemap source: Esri, HERE, Garmin Intermap, increment P Corp, GEBCO, USGS, FAO, NPS, NRCAN, GeoBase, IGN, Kadaster NL, Ordnance Survey, Esri Japan, METI, Esri China (Honk Kong), © OpenStreetMap contributors, and the GIS User Community.

Formattato: Mantieni con il successivo

Formattato: Didascalia;Figure caption;Légende italique, Giustificato

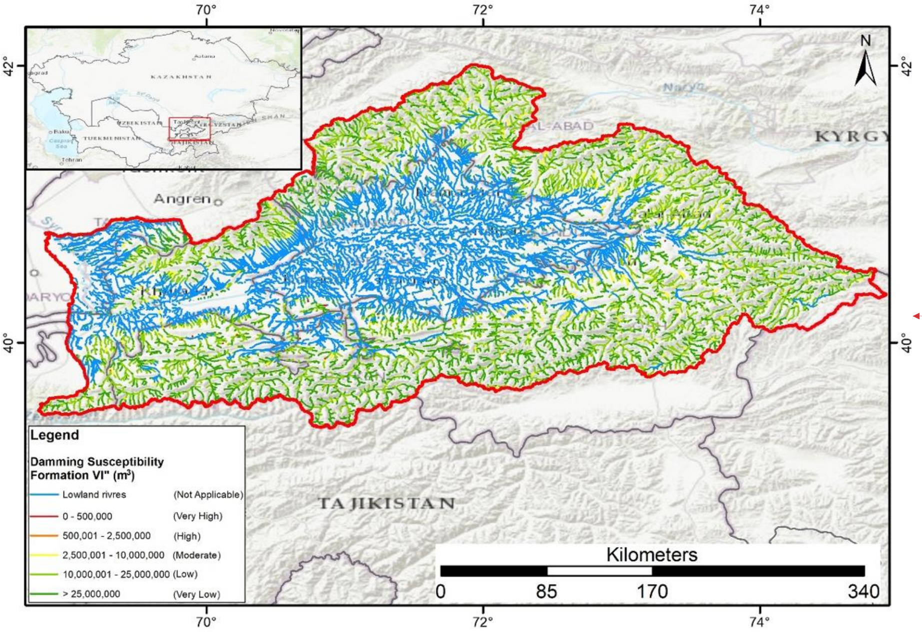

Figure 21. Damming Susceptibility Map of Formation of river stretches by new landslides in the Fergana valley

~~**Figure 28. Damming Susceptibility Map of Formation of river stretches by new landslides in the Fergana valley**~~**.** River network database from Coccia et al.~~,~~ (2023). Basemap source: Esri, HERE, Garmin Intermap, increment P Corp, GEBCO, USGS, FAO, NPS, NRCAN, GeoBase, IGN, Kadaster NL, Ordnance Survey, Esri Japan, METI, Esri China (Honk Kong), © OpenStreetMap contributors, and the GIS User Community.

5 Discussion

During the application of the damming mapping methodology, the main issues encountered was the extremely wide study area, the amount of data and the processing time required. The used mapping methodology based on the MOI equations (Eq.(1)), was originally designed to assess the damming susceptibility at basin/regional scale (Tacconi Stefanelli et al., 2016; 2020), where the morphological parameters essential for the correct application of the tool proposed by Wood (2009) must be correctly found to have an accurate river width required in the MOI equations (Eq.(1)). This time-consuming phase has been simplified in this research, according to the wide dimension of the study area, taking into account not the basins but the different states in the Central Asia region. This simplification certainly affected the reliability of the individual specific data, while still guaranteeing an important overview of the general hazard distribution of the phenomenon in the area. Furthermore, the results quality is directly proportional to the resolution and quality of the input data, which on the other hand is inversely proportional to the processing time. In this regard, a further criticality of this process is the reliability on the

Formattato: Mantieni con il successivo

Formattato: Didascalia;Figure caption;Légende italique, Giustificato

landslides volumes assessment method, since a higher quality of landslides data (sliding geometry and depth) allows the application of a more accurate volume calculation and therefore a better final result.

Considering the size of the area, in ~~Figure 11~~ Figure 9 the number of landslides classified with Very High damming predisposition (166 cases) is reasonable in absolute value, even if a bit high if compared with the total number of landslides present in the inventory (8910 cases). Without a detailed study it is not possible to say how many of these are false positives or not, however it is important to remember that this type of hazard mapping methods gives information on if and where, not when these events may occur. Although a validation of all the results is not possible, we can verify some of these through comparison with cases known in the, as shown in ~~Figure 29~~ Figure 22. These landslides have been documented in Strom (2010) who has reported several landslide dams in Central Asia regions. In Table 5 their current conditions are compared with their Damming Predisposition classification using the methodology proposed here (before the intensity reduction of the classification by one class of those landslides that intersect the river network). From this information can be observe that 23 (77% of the total) of these landslides were correctly classified with the Very High predisposition value, 1 (3%) as High and 5 (17%) with Moderate. Only one landslide, No. 22 called Arashan in Strom (2010), was classified as Low predisposition despite it obstructed the Alamedin River and then collapsed and deeply eroded. This classification error can be explained by the missing landslide volume eroded by the river as a bigger value would probably have provided a higher predisposition. Based on this simple comparison, approximately 80% of the landslide dams analysed by Strom (2010) has a corrected Damming Predisposition value (Very High) based on their volume and the width of their valley. The final classification value of Damming Predisposition of all of them has been downgraded by one class as they intersect the river network (see Section 3 Materials and Methods).

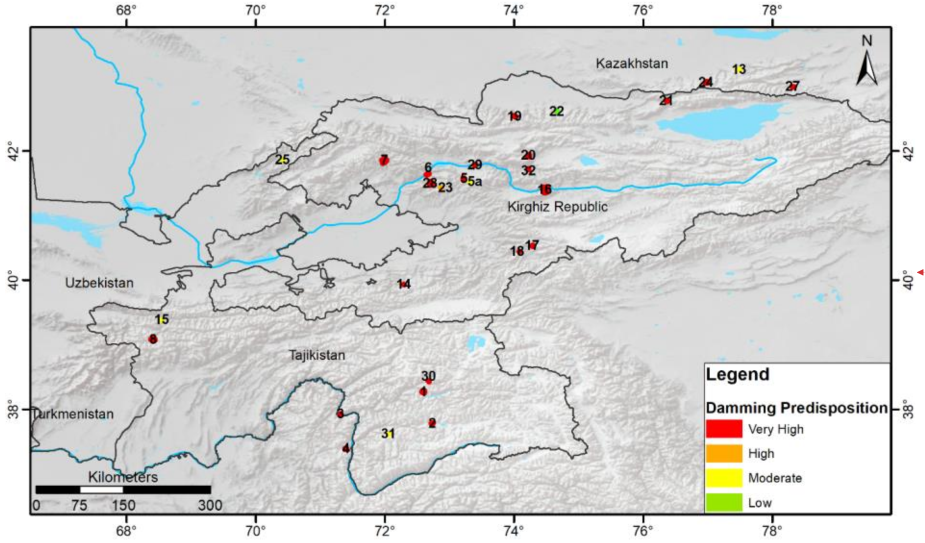

Figure 22. Map of Damming Predisposition using landslide from Strom (2010).

Formattato: Mantieni con il successivo

Formattato: Didascalia;Figure caption;Légende italique

~~Figure 29. Map of Damming Predisposition using landslide from Strom (2010).~~ See Table 5~~Table 5~~ for landslide numbers. Lake’s polygons from Esri, Garmin International, Inc.; basemap from Esri, USGS, NOAA.

ha formattato: Tipo di carattere: Non Grassetto

Table 5. Information of landslides in Figure 22~~Figure 29~~ (from Strom, 2010) and their Damming Predisposition assessment.

N.	Name	Mountain chain-Region	Consequences	Damming Predisposition
1	Usoi	Pamirs-Tajikistan	Dammed (with lake)	Very High
2	Yashilkul	Pamirs-Tajikistan	Dammed (with lake)	Very High
3	Shids	Pamirs-Tajikistan	Dammed (with lake, partially breached)	Very High
4	Shiva	Pamirs-Afghanistan	Dammed (with lake)	Very High
5	Karasu	Tien Shan-Kyrgyz Rep.	Dammed (with lake)	Very High
5a	Kapkatash	Tien Shan-Kyrgyz Rep.	Dammed (with lake)	Moderate
6	Karakul	Tien Shan-Kyrgyz Rep.	Dammed (filled lake)	Very High
7	Sarychelek	Tien Shan-Kyrgyz Rep.	Dammed (with lake)	Very High
8	Iskanderkul	Tien Shan-Tajikistan	Dammed (with lake)	Very High
9	Tianchi	Tien Shan-China	Dammed (with lake)	Very High
11	Twin-Lakes (upper)	Tien Shan-China	Dammed (with lake)	Very High
12	Twin-Lakes (lower)	Tien Shan-China	Dammed (with lake)	Very High
13	Issyk	Tien Shan-Kazakhstan	Dammed (with lake)	Moderate
14	Yashinkul	Tien Shan-Kyrgyz Rep.	Dammed (collapsed)	Very High
15	Aini	Tien Shan-Tajikistan	Dammed (lake artificially drained)	Moderate
16	Beshkiol	Tien Shan-Kyrgyz Rep.	Dammed (collapsed)	Very High
17	Kulun	Tien Shan-Kyrgyz Rep.	Dammed (with lake)	Very High
18	Kulun Mouth	Tien Shan-Kyrgyz Rep.	Dammed (filled lake)	Very High
19	Aksu	Tien Shan-Kyrgyz Rep.	Dammed (collapsed)	Very High
20	Kokomeren	Tien Shan-Kyrgyz Rep.	Dammed (collapsed)	Very High
21	Djashilkul	Tien Shan-Kyrgyz Rep.	Dammed (collapsed)	Very High
22	Arashan	Tien Shan-Kyrgyz Rep.	Dammed (collapsed)	Low
23	Kutmankul	Tien Shan-Kyrgyz Rep.	Dammed (with lake)	High
24	Bolshoe Almaty	Tien Shan-Kazakhstan	Dammed (with lake)	Very High
25	Badak	Tien Shan-Uzbekistan	Dammed (with lake)	Moderate
28	Dead Lakes	Tien Shan-Kyrgyz Rep.	Dammed (with lake)	Very High

29	Djuzumdybu-lak	Tien Shan-Kyrgyz Rep.	Dammed (with lake)	Very High
30	Kudara	Pamirs-Tajikistan	Dammed (collapsed)	Very High
31	Rivakkul	Pamirs-Tajikistan	Dammed (with lake)	Moderate
32	Ornok	Tien Shan-Kyrgyz Rep.	Dammed (collapsed)	Very High

The two maps of damming susceptibility (Figure 11~~Figure 12~~ and~~ Figure 15~~ Figure 13), while not providing probability values as done by Tacconi Stefanelli et al. (2020), offer information (the volumes of landslides) that can be more easily spent and interpreted even by operators who are not specifically expert, and for this reason have more practical utility. Furthermore, the classification of the river stretches thus produced, not requiring the alpha parameter (linked to the probability of landslide occurrence) as in the original method proposed by Tacconi Stefanelli et al. (2020), it is much easier to obtain and for this reason it can be considered an improvement within a view of wider usability.

6 Conclusions

The price of a river obstruction, in terms of reconstruction and losses on both economic and lives, can be much higher compared with the costs of a proper environmental planning and land-use management. Be able to define the areas with higher risk could considerably lower the costs, allowing to focus the economic resources in effective preventive interventions, planning and monitoring activities.

In this work a damming mapping methodology have been proposed and carried out on the Central Asia regions as a part of a multi-hazard approach in the framework of the SFRARR Project (“Strengthening Financial Resilience and Accelerating Risk Reduction in Central Asia”). The used method, originally developed applying the Morphological Obstruction Index at basin scale, have been modified to fit such a large study area and the available data. Over 8000 landslides and the entire river network of studied area have been analyzed to propose a practical tool to assess where the damming susceptibility, from reactivation of mapped landslides and formation of new landslides, are higher at national scale. The improvement of the original method allows a simpler use on a wider area, as the technical knowledge and data required can also be managed by a non-expert operator, and the need for less data, more easily available. The main limitation of the work is related to the uncertainty of the reliability of the results at local scale due to the absence of a possible validation of all results, requiring many in-depth specific studies in the areas identified with the higher predisposition. This uncertainty can be improved in future studies by using data with better resolution, coverage, and quality.

Besides its limitations, this tool can be undoubted useful in very large countries where there is a lack of diffuse assessment of landslide activity, providing preliminary information about damming susceptibility to adopt risk reduction measures, for land management and as a starting point for future studies in specific areas potentially more subject to the damming hazard identified in this work.

Code and data availability. The landslide dam mapping susceptibility method was implemented by using the cited landslide inventory maps, published by the following authors: Behling et al., 2014, 2016, 2020; Havenith et al., 2015a; Strom and Abdrakhmatov, 2018. The SRTM DEM data are available from https://earthexplorer.usgs.gov/.

The river network and other landslide inventories were provided by the SFRAAR project partners: RED (Risk, Engineering + Development – Pavia, Italy), OGS (National Institute of Oceanography and Experimental Geophysics, Seismological Research Center, Trieste, Italy), IWPHE (Institute of Water problems, Hydropower, Engineering and Ecology, Dushanbe, Republic of Tajikistan), ISASUZ (Institute of Seismology of the Academy of Science of Uzbekistan, Tashkent, Uzbekistan), LLP (Institute of Seismology of the Science Committee of the Republic of Kazakhstan, Almaty).

Author contribution. Carlo Tacconi Stefanelli implemented the damming mapping method, William Frodella conceived with Carlo Tacconi Stefanelli the article structure and collected the data, Francesco Caleca supported the method application on part of the study area. Francesco Caleca also performed statistical analysis involving the method results. All the aforementioned Authors contributed to the writing of the article and the figure graphics. Veronica Tofani coordinated the work and reviewed the paper. Zhanar Raimbekova and Ruslan Umuraliev provided environment and geomorphology information and part of the landslide database for Kazakhstan and Kyrgyz Republic.

Competing interests. The contact author has declared that none of the authors has any competing interests.

Acknowledgements. This work was developed within World Bank-funded project "*Strengthening Financial Resilience and Accelerating Risk Reduction in Central Asia*" (SFRARR), in collaboration with the European Union, and the GFDRR (Global Facility for Disaster Reduction and Recovery), with the goal of improving financial resilience and risk-informed investment planning in the central Asian countries (Kazakhstan, Kyrgyz Republic, Tajikistan, Turkmenistan and Uzbekistan). This work brings the part of the results of the Task 7 "Landslide Scenario Assessment", managed by the UNESCO Chair on Prevention and Sustainable Management of Geo-Hydrological Hazards (University of Florence, Italy). In particular, the authors would like to thank Gabriele Coccia and Paola Ceresa from Red Risk Engineering (Pavia, Italy) for providing river network data and for the valuable coordination and constant support, and also Alexander Strom and Hans Balder Havenith for providing landslide inventories and for their constructive advice and valuable observations. We would also like to thank the partners from Central Asia for the fruitful collaboration, in particular: IWPHE (Tajikistan), ISASUZ and the State Monitoring Service of the Republic of Uzbekistan for tracking dangerous geological processes (Uzbekistan), the Institute of Seismology of the National Academy of Sciences of Kyrgyz Republic (ISNASKR), and the Institute of Seismology Limited Lability Partnership (LLP) of Kazakhstan.

Financial support. This research has been supported by the World Bank Group (Consulting Services Contract No. 8006611 – Regionally consistent risk assessment for earthquakes and floods and selective landslide scenario analysis for strengthening financial resilience and accelerating risk reduction in Central Asia).

References

Abdrakhmatov, K.Y., Aldazhanov, S.A., Hager, B.H., Hamburger, M.W., Herring, T.A., Kalabaev, K.B., Makarov, P., Molnar, S.V., Panasyuk, M.T., Prilepin, R.E., Reilinger, I.S., Sadybakasov, B.J., Souter, Yu.A., Trapeznikov, V.Ye., and Tsurkov Zubovich, A.V.: Relatively recent construction of the Tien Shan inferred from GPS measurements of present-day crustal deformation rates. Nature, 384(6608), 450-45319, 1996.

Abdrakhmatov, K., Havenith, H.B., Delvaux, D., Jongmans, D., and Trefois, P.: Probabilistic PGA and Arias Intensity Maps of Kyrgyz Republic (Central Asia). J. Seismol. 7.2: 203-220, 2003.

Behling, R., Roessner, S., Kaufmann, H., and Kleinschmit, B.: Automated spatiotemporal landslide mapping over large areas using rapideye time series data. Remote Sens. 6, 8026–8055, 2014.

Behling, R., Roessner, S., Golovko, D., and Kleinschmit, B.: Derivation of long-term spatiotemporal landslide activity—A multi-sensor time series approach. Remote Sens. Environ. 186, 88–104, 2016.

Behling, R., and Roessner, S.: Multi-temporal landslide inventory for a study area in Southern Kyrgyz Republic derived from RapidEye satellite time series data (2009 – 2013). V. 1.0. GFZ Data Services. https://doi.org/10.5880/GFZ.1.4.2020.001, 2020.

Borgatti, L., and Soldati, M.: Landslides as a geomorphological proxy for climate change: a record from the Dolomites (northern Italy), Geomorphology, 120(1–2), 56–64, 2010.

CAC DRMI: Risk assessment for Central Asia and Caucasus: desk study review, 2009.

Canuti,~~.~~ P., Casagli, N., Ermini, L., Fanti, R., and Farina, P.: Landslide activity as a geoindicator in Italy: significance and new perspectives from remote sensing, Environ. Geol., 45(7), 907–919, 2004.

Casagli, N., and Ermini, L.: Geomorphic analysis of landslide dams in the Northern Apennine, Trans. Jpn. Geomorphol. Union., 20(3), 219–249, 1999.

Catani, F., Tofani, V., and Lagomarsino, D.: Spatial patterns of landslide dimension: a tool for magnitude mapping, Geomorphology 273, 361–373. https://doi.org/10.1016/j.geomorph.2016.08.032, 2016.

Chedia, O.K., and Lemzin, I.N.: Seismogenerating faults of the Chatkal depression. In: Seismotectonics and seismicity of the Tien Shan. Frunze, Ilim, 18–28, 1980.

Chen, C.~~-~~Y., Chang, J.~~-~~M.: Landslide dam formation susceptibility analysis based on geomorphic features. Landslides, 13(5), 1019-1033, 2016.

Coccia, G., Ceresa, P., Bussi, G., Denaro, S., Bazzurro, P., Martina, M., Fagà, E., Avelar, C., Ordaz, M., Huerta, B., Garay, O., Raimbekova, Z., Abdrakhmatov, K., Mirzokhonova, S., Ismailov, V., and Belikov, V.: Large-scale flood risk assessment in data scarce areas: an application to Central Asia, Nat. Hazards Earth Syst. Sci. Discuss. [preprint], https://doi.org/10.5194/nhess-2023-157, ~~in~~ under review, 2023.

Costa, J.E., and Schuster, R.L.: Documented historical landslide dams from around the world. US Geol. Surv. Open-File Report, 91(239), 1-486, 1991.

Costa, J.E., and Schuster, R.L.: Formation and failure of natural dams. Bull Geol Soc Am, 1 0 0 (7), 1054–1068. https://doi.org/10.0016-1988)100/0016-7606(1988)100<1054:TFAFON>2.3.CO, 1988.

Crozier, M.J.: Deciphering the effect of climate change on landslide activity: a review, Geomorphology, 124(3), 260–267, 2010.

Dai, F.~~-~~C., Lee, C.~~-~~F., Deng, J.~~-~~H., Tham, L.~~-~~G.: The 1786 earthquake-triggered landslide dam and subsequent dam-break flood on the Dadu River, southwestern China. Geomorphology, 65(3), 205-221, 2005.

Dal Sasso, S.F., Sole, A., Pascale, S., Sdao, F., Bateman Pinzòn, A., and Medina, V.: Assessment methodology for the prediction of landslide dam hazard, Nat. Hazards Earth Syst. Sci., 14 (3), 557–567, http://dx.doi.org/10.5194/nhess-14-557-2014, 2014.

Danneels, G., Bourdeau, C., Torgoev, I., Havenith, H.-B.: Geophysical investigation and dynamic modelling of unstable slopes: case-study of Kainama (Kyrgyzstan). Geophys. J. Int., 175(1), 17-34, 2008.

Delvaux, D., Abdrakhmatov, K.E., Lemzin, I.N., and Strom, A.L.: Landslides and surface breaks of the 1911 Ms 8.2 Kemin earthquake, Kyrgyzstan, Russian Geology and Geophysics, 2001, 42, 10, 1667-1677, 2001.

Dikau, R., and Schrott, L.: The temporal stability and activity of landslides in Europe with respect to climatic change (TESLEC): main objectives and results, Geomorphology, 30(1–2), 1–12, 1999.

Drăguţ, L., and Dornik, A.: Land-surface segmentation as a method to create strata for spatial sampling and its potential for digital soil mapping, Int. J. Geogr. Inf. Sci., 30(7), 1359-1376, 2016.

Ermini, L., Casagli, N.: Prediction of the behavior of landslide dams using a geomorphical dimensionless index, Earth Surf Proc Land 28:31–47. https://doi.org/10.1002/esp.424, 2003.

Falátková, K.: Temporal analysis of GLOFs in high-mountain regions of Asia and assessment of their causes, AUC Geographica, 51, 2, 145–154, 2016.

Fan, X., Rossiter, D.G., van Westen, C.J., Xu, Q., and Görüm, T.: Empirical prediction of coseismic landslide dam formation, Earth. Surf. Proc. Land., 39(14), 1913–1926, 2014.

Fan, X., Dufresne, A., Subramanian, S.S., Strom, A., Hermanns, R., Tacconi Stefanelli, C., Hewitt, K., Yunus, A.P., Dunning, S., Capra, L., Geertsema, M., Miller, B., Casagli, N., Jansen, J.D., and Xu, Q.: The formation and impact of landslide dams – State of the art, Earth Sci. Rev., 203, 103116, https://doi.org/10.1016/j.earscirev.2020.103116, 2020.

Fan, X., Dufresne, A., Whiteley, J., Yunus, A.-P., Subramanian, S.S., Okeke, C.-A., Pánek, T., Hermanns, R., Ming, P., Strom, A., Havenith, H.-B., Dunning, S., Wang, G., and Tacconi Stefanelli, C.: Recent technological and methodological advances for the investigation of landslide dams, Earth-Sci. Rev., 218, 103646, https://doi.org/10.1016/j.earscirev.2021.103646, 2021.

Farr, T.G., and Kobrick, M.: Shuttle Radar Topography Mission produces a wealth of data. Eos Trans. AGU, 81, 583-583, 2000.

Golovko, D., Roessner, S., Behling, R., Wetzel, H.-U., and Kleinschmidt, B.: Development of multi-temporal landslide inventory information system for southern Kyrgyz Republic using GIS and satellite remote sensing, PFG, 2015(2), 157–172, 2015.

Guzzetti, F., Ardizzone, F., Cardinali, M., Rossi, M., and Valigi, D.: Landslide volumes and landslide mobilization rates in Umbria, central Italy, EPSL, 279, 222–229, 2009.

Havenith, H.B., Strom, A., Cacerez, F., and Pirard, E.: Analysis of landslide susceptibility in the Suusamyr region, Tien Shan: statistical and geotechnical approach. Landslides 3, 39–50, 2006a.

Havenith, H.B., Torgoev, I., Meleshko, A., Alioshin, Y., Torgoev, A., and Danneels, G.: Landslides in the Mailuu-Suu Valley, Kyrgyz Republic—hazards and impacts, Landslides, 3, 137–147, 2006b.

Havenith, H.B., Strom, A., Torgoev, I., Torgoev, A., Lamair, L., Ischuk, A., and Abdrakhmatov, K.: Tien Shan geohazards database: Earthquakes and landslides, Geomorphology, 249, 16–31, 2015a.

Havenith, H.B., Torgoev, A., Schlögel, R., Braun, A., Torgoev, I., and Ischuk, A.: Tien Shan geohazards database: Landslide susceptibility analysis, Geomorphology, 249, 32–43, 2015b.

Havenith, H.B., Umaraliev, R., Schlögel, R., Torgoev, I., Ruslan, U., Schlogel, R., and Torgoev, I.: Past and Potential Future Socioeconomic Impacts of Environmental Hazards in Kyrgyz Republic. In Kyrgyz Republic: Political, Economic and Social Issues; Olivier, A.P., Ed.; Nova Science Publishers, Inc.: Hauppauge, NY, USA; pp. 63–113, 2017.

Hungr, O., and Evans, S.G.: Entrainment of debris in rock avalanches: an analysis of a long run-out mechanism, Geol. Soc. Am. Bull., 116(9-10), 1240-1252, 2004.

Juliev, M., Pulatov, A., and Hubl, J.: Natural hazards in mountain regions of Uzbekistan: A review of mass movement processes in Tashkent province. International Journal of Scientific and Engineering Research, 8(2), 1102, 2017.

Kalmetieva, Z.A., Mikolaichuk, A.V, Moldobekov, B.D., Meleshko, A.~~-~~V, Janaev, M.M., and Zubovich, A.V.: Atlas of earthquakes in Kyrgyz Republic. Central-Asian Institute for Applied Geosciences and United Nations International Strategy for Disaster Reduction Secretariat Office in Central Asia, Bishkek, p 75, 2009.

King, J., Loveday, I., Schuster, R.~~-~~L.: The 1985 Bairaman landslide dam and resulting debris flow, Papua New Guinea. Q J Eng Geol Hydroge, 22(4), 257-270, 1989.

Kropáček, J., Vilímek, V., ~~&~~ and Mehrishi, P.: A preliminary assessment of the Chamoli rock and ice avalanche in the Indian Himalayas by remote sensing, Landslides, 18, 3489–3497, https://doi.org/10.1007/s10346-021-01742-1, 2021.

Liao, H.~~-~~M., Yang, X.~~-~~G., Lu, G.~~-~~D., Tao, J., and Zhou, J.~~-~~W.: A geotechnical index for landslide dam stability assessment, Geomatics, Natural Hazards and Risk, 13(1), 854-876, https://doi.org/10.1080/19475705.2022.2048906, 2022.

Maxwell, A.E., and Shobe, C.M.: Land-surface parameters for spatial predictive mapping and modeling, Earth-Sci. Rev., 226, 103944, 2022.

Molnar, P., and Tapponnier, P.: Cenozoic Tectonics of Asia: Effects of a Continental Collision: Features of recent continental tectonics in Asia can be interpreted as results of the India-Eurasia collision. science, 189(4201), 419-426, 1975.

Niyazov, R.A.: Uzbekistan landslides. Uzbekistan landslide service. Technical report, 2020.

Peresan, A., Scaini, C., Tyagunov, S., and Ceresa, P.: Capacity Building Experience for Disaster Risk Reduction in Central Asia, Nat. Hazards Earth Syst. Sci. Discuss. [preprint], https://doi.org/10.5194/nhess-2023-156, in review, 2023.

Persits, F.M., Ulmishek, G. F., Steinshouer, D.W.: Maps showing geology, oil and gas fields and geologic provinces of the Former Soviet Union (No. 97-470-E). US Geological Survey, https://doi.org/10.3133/ofr97470E, 1997.

Petrov, M.A., Sabitov, T.Y., Tomashevskaya, I.G., Glazirin, G.E., Chernomorets, S.S., Savernyuk, E.A., Tutubalina O.V., Petrakov, D.A., Sokolov, L.S., Dokukin, M.D., Mountrakis, G., Ruiz-Villanueva, V., and Stoffel, M.: Glacial lake inventory and lake outburst potential in Uzbekistan, Sci. Total Environ., 592, 228-242, 2017.

Piroton, V., Schlögel, R., Barbier, C., and Havenith, H.B.: Monitoring the recent activity of landslides in the Mailuu-suu valley (Kyrgyz Republic) using radar and optical remote sensing techniques. Geosciences, 10 (5), p. 164, 2020.

Popescu, M.E., and Sasahara, K.: Engineering Measures for Landslide Disaster Mitigation, in: Landslides – Disaster Risk Reduction, edited by: Sassa, K., Canuti, P., Springer, Berlin, Heidelberg, 609-631, https://doi.org/10.1007/978-3-540-69970-5_32, 2009.

Righini, M., and Surian, N.: Remote sensing as a tool for analysing channel dynamics and geomorphic effects of floods, Flood monitoring through remote sensing, 27-59, 2018.

Rosi, A., Frodella, W., Nocentini, N., Caleca, F., Havenith, H.B., Strom, A., Saidov, M., Bimurzaev, G.A., and Tofani, V.: Comprehensive landslide susceptibility map of Central Asia, Nat. Hazards Earth Syst. Sci., 23, 2229–2250, https://doi.org/10.5194/nhess-23-2229-2023, 2023.

Saponaro, A., Pilz, M., Wieland, M., Bindi, D., Moldobekov, B., and Parolai, S.: Landslide susceptibility analysis in data-scarce regions: the case of Kyrgyz Republic. Bull. Eng. Geol. Environ. 74, 1117–1136, 2014.

Schlögel, R., Torgoev, I., De, Marneffe, C., and Havenith, H.B.: Evidence of a changing size-frequency distribution of landslides in the Kyrgyz Tien Shan, Central Asia. Earth Surf Process Landf 36(12), 1658–1669, 2011.

Schuster, R.L., and Evans, S.G.: Engineering Measures for the Hazard Reduction of Landslide Dams, in: Natural and Artificial Rockslide Dams. Lecture Notes in Earth Sciences, edited by: Evans, S., Hermanns, R., Strom, A., Scarascia-Mugnozza, G., Springer, Berlin, Heidelberg, https://doi.org/10.1007/978-3-642-04764-0_2, 2011.

Semakova, E., Gunasekara, K., and Semakov, D.: Identification of the glaciers and mountain naturally dammed lakes in the Pskem, the Kashkadarya and the Surhandarya River basins, Uzbekistan, using ALOS satellite data, Geomat. Nat. Hazards Risk, 7(3), 1081-1098, 2016.

Styron, R., Pagani, M.: The GEM Global Active Faults Database." Earthquake Spectra, vol. 36, no. 1_suppl, Oct. 2020, pp. 160–180, https://doi.org/10.1177/8755293020944182, 2020.

Strom, A.: Landslide dams in Central Asia region. Journal of the Japan Landslide Society, 47(6), 309-324, 2010.

Strom, A., and Abdrakhmatov, K.: Large-Scale Rockslide Inventories: From the Kokomeren River Basin to the Entire Central Asia Region (WCoE 2014–2017, IPL-106-2, in: Workshop on World Landslide Forum. Springer, Cham, pp. 339–346, 2017.

Strom, A., and Abdrakhmatov. K.: Rockslides and rock avalanches of Central Asia: distribution, morphology, and internal structure. Elsevier, 441pg. ISBN: 978-0-12-803204-6, 2018.

Swanson, F.J., Oyagi, N., and Tominaga, M.: Landslide dams in Japan, in: Landslide dams: processes, risk and mitigation, vol 3, edited by: Schuster R.L., Geotech. Sp., ASCE, New York, 131–145, 1986.

Tacconi Stefanelli, C., Catani, F., Casagli, N.: Geomorphological investigations on landslide dams. Geoenv Disast 2(1):1–15. https://doi.org/10.1186/s40677-015-0030-9, 2015.

Tacconi Stefanelli, C., Segoni, S., Casagli, N., and Catani, F.: Geomorphic indexing of landslide dams evolution, Eng. Geol., 208, 1–10. https://doi.org/10.1016/j.enggeo.2016.04.024, 2016.

Tacconi Stefanelli, C., Vilímek, V., Emmer, A., and Catani, F.: Morphological analysis and features of the landslide dams in the Cordillera Blanca, Peru, Landslides, 15(3), 507-521, https://doi.org/10.1007/s10346-017-0909-5, 2018.

Tacconi Stefanelli, C., Casagli, N., and Catani, F.: Landslide damming hazard susceptibility maps: a new GIS-based procedure for risk management, Landslides, 17, 1635-1648, https://doi.org/10.1007/s10346-020-01395-6, 2020.

Trifonov, V.G., Makarov, V.I., and Scobelev, S.F.: The Talas-Fergana active right-slip faults. Ann Tectonicae 6:224–237, 1992.

Ullah, S., Bindi, D., Pilz, M., Danciu, L., Weatherill, G., Zuccolo, E., Anatoly Ischuk, A., Mikhailova, N.N., Abdrakhmatov, K., and Parolai, S.: Probabilistic seismic hazard assessment for Central Asia. Annals of Geophysics, 58(1), 2015.

Wang, X., Ding, Y., Liu, S., Jiang, L., Wu, K., Jiang, Z., and Guo, W.: Changes of glacial lakes and implications in Tian Shan, central Asia, based on remote sensing data from 1990 to 2010, Environ. Res. Lett., 8(4), 044052, 2013.

Wang, D., Laffan, S.W., Liu, and Y., and Wu, L.: Morphometric characterization of landform from DEMs, Int. J. Geogr. Inf. Sci., 24(2), 305–326, 2010.

Wood, J.: Geomorphometry in LandSerf. In: Hengl, T. and Reuter, H.I. [Eds.]: Geomorphometry: Concepts, Software, Applications, Dev. Soil. Sci., 33, 333-349, 2009.

Zubovich, A.-V., Wang, X.-Q., Scherba, Y.-G., Schelochkov, G.-G., Reilinger, R., Reigber, C., Mosienko, O., Molnar, P., Michajljow, W., Makarov, V.I., Li, J., Kuzikov, S.I., Herring, T.A., Hamburger, M.W., Hager B.H., Dang, Y., Bragin, V.D., and Beisenbaev, R.: GPS velocity field for the Tien Shan and surrounding regions. Tectonics, 29(6), 2010.